Early Transition Metal Promoted Reductive CO Coupling. Mechanistic Details of Zirconocene Enediolate Formation from Isotope Crossover Experiments and Molecular Orbital Studies

Peter Hofmann*[a], Peter Stauffert[a], Martin Frede[a], and Kazuyuki Tatsumi*[b]

Anorganisch-chemisches Institut der Technischen Universität München[a], Lichtenbergstraße 4, D-8046 Garching, FRG

Department of Macromolecular Science, Faculty of Science, Osaka University[b], Toyonaka, Osaka 560, Japan

Received February 23, 1989

Key Words: CO coupling / Organometallic reaction mechanisms / Applied MO theory / Zirconocene chemistry / η^2-Ketone complexes

Molecular orbital calculations together with an isotope crossover study provide insight into mechanistic details of enediolate-forming early transition metal promoted reductive CO coupling reactions. It is shown by deuterium labeling, that Bercaw's carbonylation of $Cp^*_2Zr(CH_3)_2$ (**1**), which directly leads to the enediolate complex **2**, is an exclusively intramolecular process. Both methyl groups and the two CO molecules of **2** assemble at a single Zr center. MO investigations for $Cp_2Zr(CH_3)_2$ as a model of **1** reveal that such group 4 metallocene-promoted enediolate-producing reactions do not involve the proposed intramolecular coupling of two acyl ligands of a bis(acyl) complex generated by double CO insertion, as found for actinide derivatives. Based upon related available experimental evidence and the electronic structure of the monoinsertion product $Cp_2Zr(COCH_3)(CH_3)$, an alternative mechanism for enediolate formation is suggested and tested by extensive MO calculations. The postulated keystep consists of a methyl to acetyl migration in $Cp_2Zr(COCH_3)(CH_3)$ leading to an η^2-acetone intermediate $Cp_2Zr(\eta^2$-acetone) (**30**). Interestingly, the methyl-acetyl bond formation in model calculations requires a prohibitively high energy, unless it is assisted by an additional electron donor at the metal during the transfer of the CH_3 group to the acetyl carbon. Using a CO molecule as an incoming model nucleophile, a low energy pathway is found, which can lead from $Cp_2Zr(COCH_3)(CH_3)$ to a zirconaoxirane intermediate **36** (an η^2-acetone complex), carrying an additional stabilizing CO ligand. Subsequent CO insertion in **36** and further rearrangement opens a reaction channel towards the enediolate monomer. The overall mechanistic picture emerging from this experimental/theoretical study is consistent with recent results of the Bercaw group, which has actually isolated the postulated intermediates of type **36**. The electronic differences between the systems treated here and corresponding actinide or bis(aryloxy) analogs are briefly discussed.

Durch frühe Übergangsmetalle induzierte CO-Kopplungsreaktionen. – Mechanistische Untersuchung der Zirkonocen-Endiolat-Bildung mit Hilfe von Isotopenmarkierungs-Kreuzungsexperimenten und Molekülorbital-Berechnungen

MO-Modellrechnungen und ein Isotopenmarkierungs-Kreuzungsexperiment erlauben Einblick in mechanistische Details reduktiver, von frühen Übergangsmetallen induzierter CO-Kopplungsreaktionen. Durch Deuteriummarkierung wird gezeigt, daß die von Bercaw aufgefundene Carbonylierung von $Cp^*_2Zr(CH_3)_2$ (**1**), die direkt den Endiolatkomplex **2** liefert, ein ausschließlich intramolekularer Prozeß ist. Beide Methylgruppen und die zwei CO-Moleküle vereinigen sich an einem einzigen Zr-Zentrum. MO-Untersuchungen am Modell $Cp_2Zr(CH_3)_2$ erweisen, daß derartige Endiolat-bildende Reaktionen in Metallocenderivaten der 4. Gruppe nicht über die vermutete intramolekulare Kopplung zweier Acylliganden eines durch doppelte CO-Insertion intermediär entstandenen Bis(acyl)-Komplexes verlaufen, wie es bei analogen Actinidensystemen der Fall ist. Auf der Grundlage verfügbarer Experimentalbefunde und aus der Elektronenstruktur des Monoinsertionsproduktes $Cp_2Zr(COCH_3)(CH_3)$ wird ein alternativer Endiolat-Bildungsweg abgeleitet und durch umfangreiche MO-Berechnungen getestet. Sein entscheidender Schritt besteht in einer von $Cp_2Zr(COCH_3)(CH_3)$ ausgehenden Methyl-Acetyl-Kopplung, die zum η^2-Acetonkomplex $Cp_2Zr(\eta^2$-aceton) (**30**) als vorgschlagenem Intermediat führt. Die Modellrechnungen zeigen jedoch eine unerwartet hohe, prohibitive Energiebarriere für den Kopplungsschritt von Methyl- und Acetylgruppe, wenn die Übertragung der CH_3-Gruppe auf den Acetylkohlenstoff nicht simultan durch einen eintretenden Donorliganden am Metall unterstützt wird, der zusätzliche Elektronendichte zur Verfügung stellt. Mit einem CO-Molekül als eintretendem Modell-Nucleophil ergibt sich ein energetisch günstiger Reaktionsweg, der von $Cp_2Zr(COCH_3)(CH_3)$ zu einem Zirconaoxiran **36** (einem η^2-Acetonkomplex) als Zwischenprodukt führen kann, das einen zusätzlichen, stabilisierenden CO-Liganden enthält. Nachfolgende CO-Insertion in **36** und Umlagerung eröffnen einen plausiblen Reaktionskanal zum monomeren Endiolat-Endprodukt. Das aus dieser kombiniert experimentell/theoretischen Arbeit sich ergebende mechanistische Gesamtbild stimmt mit neueren Resultaten der Bercawschen Gruppe überein, in denen die Beteiligung der postulierten Zwischenstufen vom Typ **36** durch Isolierung nachgewiesen wurde. Elektronische Unterschiede zwischen den hier behandelten Systemen und entsprechenden Actiniden- oder Bis(aryloxy)-Analoga werden kurz diskutiert.

  0009–2940/89/0808–1559 $ 02.50/0

The transition metal mediated catalytic or stoichiometric formation of carbon–carbon bonds involving carbon monoxide, one of the most important C_1 resources, continues to be a prominent research topic in organic and organometallic chemistry[1]. CO insertion reactions into transition metal carbon bonds, which often result in further transformations, have been extensively studied both by theory and by experiment[2]. During the last decade, a variety of carbon monoxide-based stoichiometric C–C bond-forming processes, starting out from early transition metal organometallics, has been uncovered[3]. Although most of them are not catalytic themselves, they are believed to serve as useful model reactions for various steps in homogenous or heterogeneous catalytic CO chemistry. Be that as it may, transition metal promoted stoichiometric, highly specific, multicomponent assembly reactions, yielding complex organic molecules in one-pot procedures, are of sufficient interest in their own right.

One of the most remarkable C–C coupling reactions in the field of early transition metal chemistry has been discovered by the Bercaw group in 1978[4a] and is shown in Scheme 1.

Scheme 1

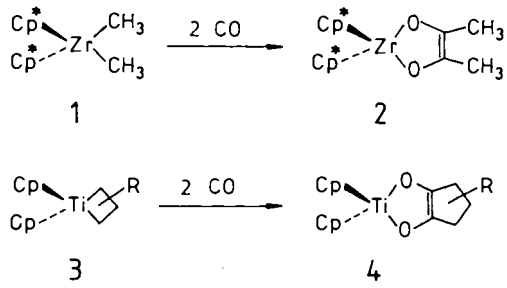

Treatment of the permethylzirconocene derivative $Cp^*_2Zr(CH_3)_2$ (**1**) [$Cp^* = \eta^5$-$C_5(CH_3)_5$] with CO directly yields **2**, a monomeric enediolate complex of permethylzirconocene. This fascinating transformation, irrespective of its actual mechanism, formally represents a doubly alkylating, reductive coupling of 2 CO molecules, selectively connecting four C_1 fragments in a single synthetic step under very mild conditions! Analogous enediolate monomer formation reactions have also been found for permethylhafnocene derivatives[5], for other organyl groups than CH_3[6], for alkyl hydrides of Cp^*_2Zr and Cp^*_2Hf and, at reaction temperatures as low as −50°C, for various bis(cyclopentadienyl)-titanacyclobutanes[7], as shown in Scheme 1 (**3** → **4**). Oxidative degradation of monomeric enediolates like **2** or **4** yields 1,2-diketones, acid hydrolysis gives rise to the corresponding acyloins. So these CO/alkyl coupling reactions (in particular with unsymmetrical group 4 metallocene bis-organyl derivatives) may well be of future synthetic utility[8].

It is apparent, that transformations like **1** → **2** or **3** → **4** must involve several and possibly rather complex mechanistic steps. A large body of experimental background concerning the CO chemistry of early transition metal organometallics is already available and has led to plausible suggestions about the mechanistic pathway from, e.g., **1** to **2**. Still however, different routes towards the final products represented in Scheme 1 can be inferred and no clear-cut conclusion has been drawn yet.

Without further going into details here we note, that enediolate formation by carbonylation has recently been observed also for actinide[9] and for bis(aryloxy)zirconium bis-organyl systems[10]. There, some mechanistic work has been published, but, as will be discussed later (vide infra), these seemingly identical reductive CO (or isocyanide) coupling reactions apparently do not follow the same mechanism which we find for group 4 metallocene derivatives in our experimental and theoretical work reported.

It is the purpose of this paper, to adress some crucial aspects of group 4 metallocene-promoted reductive CO coupling reactions by both experimental (isotope crossover) and molecular orbital (Extended Hückel MO) investigations.

Experimental and Theoretical Background

Experimental efforts to isolate intermediates of the two reactions shown in Scheme 1 have so far been unsuccessful. From the chemistry of $Cp^*_2Zr(CH_3)_2$ it is clear, however, that the initial step of the **1** to **2** transformation is a CO insertion into one of the $Zr-CH_3$ bonds. We have reported an extensive molecular orbital investigation of the carbonylation chemistry of $Cp_2Zr(CH_3)_2$[11a,b], and we summarize briefly its results here, because they are essential for the following analysis. As shown in Scheme 2, carbon monoxide inserts through a "*lateral*" (as opposed to "central") attack with a very low energy of activation[11c,d], and its regioselectivity is controlled by orbital symmetry [HOMO CO/LUMO $Cp_2Zr(CH_3)_2$].

Scheme 2

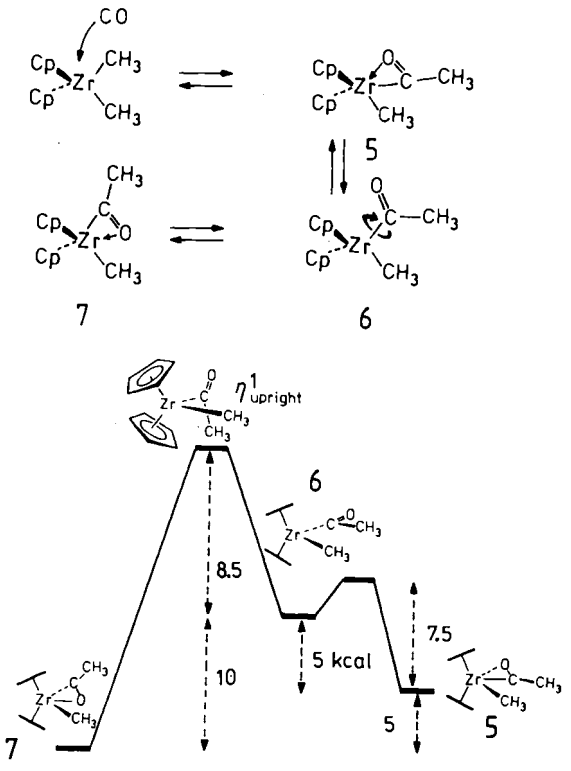

In agreement with low temperature spectroscopic studies by Erker et al.[12], kinetically controlled CO insertion is calculated to lead to the "O-outside" η^2-acyl structure **5**, which, according to the computed energy profile in Scheme 2, can easily detach its oxygen atom from the Zr center (an "O-outside" η^1-acyl system **6** appears as a local minimum on the energy surface for acyl coordination[13]). Unlike the η^2-acetyl ligand of **5**, the resulting η^1-CH_3CO group is able to rotate around the Zr–CO bond. Passing a maximum energy point with an upright acyl the "O-inside" structure **7** is finally reached. It represents the thermodynamic product of the CO insertion process[14]. Our computed barrier[11b] for "O-outside" to "O-inside" isomerization of $Cp_2Zr(\eta^2\text{-}COCH_3)(CH_3)$ (ca. 13 kcal/mol) compares extremely well with Erker's experimental value of $\Delta G = 11$ kcal/mol[12a]. Isolation of CO insertion products, if possible, in each case gave the more stable "O-inside" isomers, which were characterized by X-ray analysis in a few cases[15].

Returning back to enediolate formation from **1** (Scheme 1) we thus can safely assume, that its first mechanistic step has to be mono-insertion of CO to form $Cp^*_2Zr(\eta^2\text{-}COCH_3)(CH_3)$. Indeed, this species has been identified spectroscopically by Bercaw and co-workers[4a] in solution. $Cp^*_2Zr(\eta^2\text{-}COCH_3)(CH_3)$, unlike $Cp_2Zr(\eta^2\text{-}COCH_3)(CH_3)$, could not be isolated because of very facile CO deinsertion and its high solubility. In analogy to the findings described above, η^2-"O-inside" acetyl coordination in $Cp^*_2Zr(\eta^2\text{-}COCH_3)(CH_3)$ can be expected to occur at room temperature, although this has not been proven. Given the low barrier of "O-inside" → "O-outside" interconversion, this point is of no great significance for our following discussion. It is essential, however, that the preformed $Cp^*_2Zr(\eta^2\text{-}COCH_3)(CH_3)$ can be further carbonylated in a second reaction step, yielding the enediolate complex **2** under identical conditions as used for converting **1** to **2** directly.

A tentative reaction mechanism for enediolate formation, involving $Cp^*_2Zr(\eta^2\text{-}COR)(R)$ species as first intermediates was originally proposed by Bercaw et al.[4a] and is shown in Scheme 3.

Scheme 3

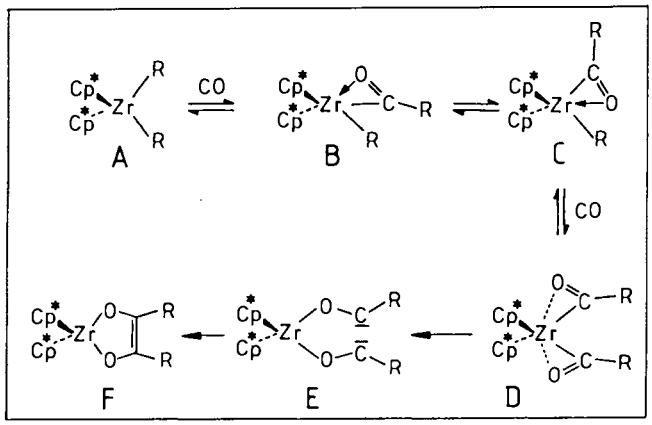

According to this proposal, mono-insertion of CO would be followed by a second insertion step into the other Zr–carbon bond, generating a bis-acyl complex **D**. Because of facile "O-outside" → "O-inside" interconversions (viz. **B** → **C**) of η^2-acyl ligands via η^1 structures, an intermediate geometric situation might be accessible, in which both in-plane COR groups are oriented "O-outside" and can rearrange more or less synchronously, attaching their oxygens to the metal and simultaneously coupling their carbon atoms as indicated in Scheme 3 (**D** → **E** → **F**). The bis-zirconoxycarbene structure **E** does not have to be an intermediate but could just be a waypoint on the overall downhill energy surface carrying **D** towards the enediolate structure **F**.

The most important aspect of this mechanism lies in its assumption of consecutive double insertion and bis-acyl formation as a necessary condition for an intramolecular, metal-centered, more or less "concerted" ligand reorganization process, which in fact has an analog in Th chemistry[9].

Encouraged by previous experiences with EH MO model calculations for CO insertion and acyl coordination modes in zirconocene and titanocene species[11a,b], we therefore decided to study the proposed enediolate-forming pathway and conceivable mechanistic alternatives theoretically, using $Cp_2Zr(CH_3)_2$ as a model[16].

Before we begin to report the results of our computational investigations, we must digress shortly in order to address a crucial question which had to be answered before any molecular orbital studies were begun. Up to this point we have tacitly assumed, that monomeric enediolate complexes (**2**, **F**) are formed through *intra*molecular pathways at a single Zr center. We have not considered mechanistic routes through bimolecular processes, which obviously would limit or complicate the chances to reach mechanistic insight by MO calculations. The titanacyclobutane transformation **3** → **4** of Scheme 1 of course only seems consistent with an *intra*molecular reaction at a single titanium. Unfortunately, things are less clear-cut for Cp_2Zr or Cp^*_2Zr derivatives (**1**, **A**) with two independent R groups. Experimental evidence does exist for *inter*molecular reaction sequences leading to enediolate structures. The carbonylation of the chlorohydride $Cp_2Zr(Cl)(H)$ (**8**) is particularly relevant in this context. Floriani has shown[17], that **8** can be doubly carbonylated to yield the unsubstituted enediolate complex dimer **11** and Cp_2ZrCl_2 (Scheme 4).

Scheme 4

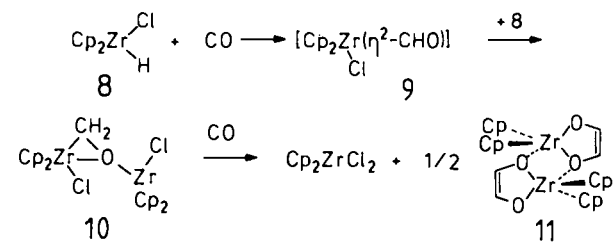

A binuclear intermediate **10** was isolated and has been structurally characterized by X-ray crystallography. The initial formation of a formyl complex **9** (probably with η^2-bound CHO) by CO insertion into the Zr–H bond, followed by *inter*molecular hydride transfer from a second mol-

ecule of **8** to the strongly electrophilic (carbenium-like[11b]) formyl carbon, yielding **10**, has been postulated. Further carbonylation, elimination of Cp_2ZrCl_2, rearrangement, and dimerization finally result in **11**. We will come back to a detailed description of the steps between **10** and **11** later, but we must note here, that an entirely analogous bimolecular mechanism with both enediolate ring substituents R (e.g. of **2** or **F**) *not* originating from the same metal center could in principle be written for $Cp_2Zr(CH_3)_2$ or $Cp^*_2Zr(CH_3)_2$ as well. Both R groups, like the two enediolate hydrogens of **11**, would then stem from different Zr atoms. Instead of Cp_2ZrCl_2 as in Scheme 4, the respective dimethyl compound would be formed and would reenter the carbonylation sequence, finally yielding the enediolate product **2** exclusively, as is observed. The *inter*molecular transfer of a Zr-bound methyl group or hydride ligand to an η^2-acyl group of a second molecule has been reported independently[3b,18] and is fully consistent with the electronic structure[11b] of η^2-acyl groups in bonding situations as discussed here.

To eliminate the prohibitive need of performing model MO calculations also for binuclear species and for *inter*molecular variants of enediolate formation processes, we considered it mandatory to test the *intra*- vs. *inter*molecular nature of the actual **1** → **2** reaction experimentally.

Crossover Carbonylation Study

The *intra*molecular nature of enediolate formation for actinide dialkyls $Cp^*_2AnR_2$ (An = Th or U) has been recently established[9] by a ^{13}C labeling crossover carbonylation experiment with a 1:1 mixture of $Cp^*_2Th(CH_3)_2$ and $Cp^*_2Th(^{13}CH_3)_2$. ^{13}C labeling was necessary because of hydrolytic workup with acid, which would have made deuterium labeling of the resulting acyloin methyl groups useless. We chose $Cp^*_2Zr(CH_3)_2$ (**1**) and its deuterated analog $Cp^*_2Zr(CD_3)_2$ (**1-d$_6$**) for our crossover carbonylation study, because the known volatility of Cp^*_2Zr-enediolate complex **2** was expected to allow the analysis of product isotope distribution patterns by mass spectrometry without the need for acid cleavage and acyloin isolation. The synthesis of $Cp^*_2Zr(CD_3)_2$ from $Cp^*_2ZrCl_2$ and CD_3Li was straightforward and carbonylation of a 1:1 mixture of **1** and **1-d^6** as well as of both isotopomers alone was conducted as described in the experimental part and in accord with Bercaw's original paper[4a].

Scheme 5

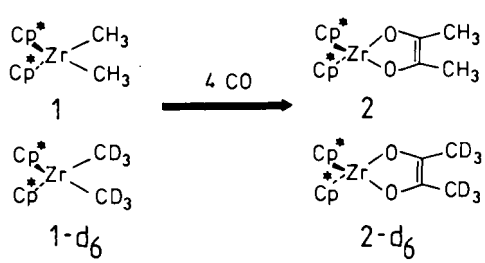

Strictly *intra*molecular reductive coupling, neglecting kinetic isotope effects, should lead to a 1:1 mixture of enediolate complexes with only CH_3 or CD_3 groups (**2-d$_0$**, **2-d$_6$**) without formation of the mixed CH_3/CD_3 product **2-d$_3$**, as shown in Scheme 5. Exclusively *inter*molecular product formation would lead to a 1:2:1 mixture of **2-d$_0$**, **2-d$_3$**, and **2-d$_6$**. Our experimental result is only consistent with an entirely *intra*molecular reaction. Taking into account the natural isotope distribution of Zr and carbon and the 99% deuterium labeling of the CD_3Li (CD_3I) used, the isotopic mass distribution pattern of the molecular ion peaks in mass spectra of the isolated enediolate complex mixture shows only less than 0.5% of the CH_3/CD_3 species **2-d$_3$** to be present. Within experimental error, enediolate formation thus occurs at a single metal center. Molecular orbital model studies involving only mononuclear species and a single Cp_2Zr unit seemed reasonably justified.

The Bis-acyl Coupling Pathway

In close analogy to our previous analysis[9] for coupling two acyl ligands in $Cp^*_2An(\eta^2\text{-acyl})_2$ actinide systems, we start our theoretical analysis by inspecting the originally proposed and seemingly "least complicated" pathway for enediolate formation, i.e. a concerted, least motion, in-plane coupling of two Zr-coordinated acetyl groups in $Cp_2Zr(COCH_3)_2$ (**D** in Scheme 3), first retaining C_{2v} symmetry throughout. A groundstate ligand rearrangement along

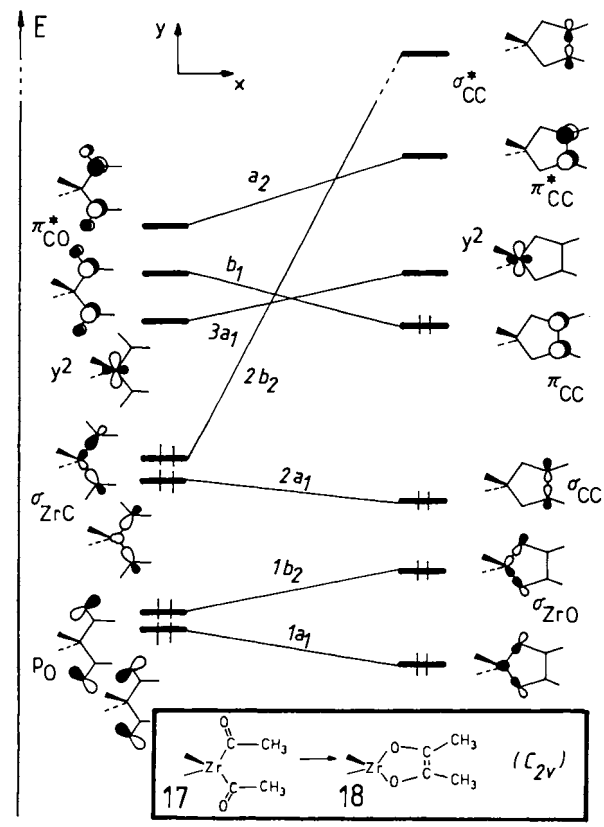

Figure 1. Schematic orbital correlation diagram for a least motion (C_{2v}) coupling of two acetyl ligands, taking $Cp_2Zr(COCH_3)_2$ (**17**, η^1-η^1) to the corresponding enediolate complex. Only the relevant levels, correlations, and contributions to the starting compound and product wave functions are shown, Cp ligands are omitted for clarity. For details see text

D → **E** → **F**, whatever its geometric details along the reaction coordinate may be, at some point necessarily encounters a situation similar to a head-to-head approach of two singlet methylenes and, accordingly, must be suspected to exhibit the electronic features of a symmetry-forbidden reaction, unless the presence of the metal center changes things[19]. It is easy to construct a Woodward-Hoffmann-type orbital correlation diagram for a least motion path (C_{2v}) of acyl coupling in $Cp_2Zr(COCH_3)_2$. This orbital correlation diagram, based upon MO model calculations, is shown schematically in Figure 1.

As indicated in the diagram, a bis(η^1-$COCH_3$) ligand coordination mode with both carbonyl group oxygens located "O-outside" is chosen to allow a smooth C_{2v} transit to the enediolate ring. Before entering the discussion of Figure 1, we have to comment upon this choice briefly. As mentioned above, acyl groups are known to prefer η^2-coordination in group 4 metallocene derivatives. We have shown[9] that the minimum energy structure for bis-acyl complexes, e.g. $Cp_2Ti(COCH_3)_2$, is in fact of the mixed η^1-η^2-type, making up for a formal 18-valence electron count at the metal. Four different in-plane η^1-η^2-bis-acyl structures are then possible for $Cp_2Zr(COCH_3)_2$, which are depicted in **12** – **15** of Scheme 6. The oxygen atoms, both of the η^1- or the η^2-bound acetyl group, may adopt either an "O-inside" or an "O-outside" orientation.

Scheme 6

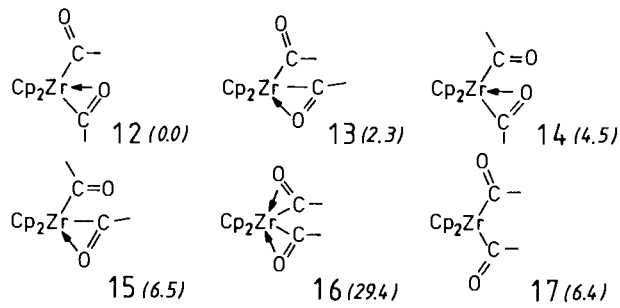

The intended evaluation of a synchronous acyl coupling pathway according to Figure 1 requires some knowledge about these different coordination modes of a bis-acetyl ligand set. The numbers in parentheses in Scheme 6 give the relative energies (kcal/mol) of the structures shown, as they result from a restricted geometry optimization (see Appendix) in each case, minimizing the energy for a given η^1- and/or η^2-combination of the acyl ligand pair. As expected from the analysis of monoacyl species[11a,b], isomer **12** with one "O-inside" η^2-acetyl group and with the second acyl group η^1-bound, is found at lowest energy, but all the four 18-electron η^1-η^2 structures lie within an energy range of only 6 – 7 kcal/mol. Their interconversion by means of rotating an η^1-CH_3CO ligand around the Zr – C bond (viz. Scheme 2) is facile[20]. In particular, we note that **17** the η^1-η^1 isomer with both oxygens "O-outside", is also easily accessible, bringing us back to Figure 1, where it represents the starting compound side of the correlation diagram. For **17**, both Zr – O distances are 299.2 pm, the two acyl carbons are 368.5 pm apart, the Zr – C_{COCH_3} bonds are 219.7 pm. At left in Figure 1, the relevant symmetry-adapted orbitals of η^1-η^1-$Cp_2Zr(COCH_3)_2$ are qualitatively shown, displaying only the main contributions to each wave function. In ascending energetic order, these are the two p-type oxygen lone pair MOs of the carbonyl groups (their in-phase and out-of-phase linear combinations), followed by the two highest occupied MOs of the complex, representing the two Zr – C bonds. The two low-lying unoccupied levels of π^*_{CO} character are located just above the "y^2" empty metal d-orbital, the typical LUMO for d^0-Cp_2ML_2 systems[21]. The right side of Figure 1 gives the corresponding valence MOs of the planar C_{2v} enediolate system. From top to bottom there is the newly formed C – C σ^*-MO of the enediolate ring, not drawn to scale at very high energy, the C – C π^* orbital, again the "y^2" empty d-orbital at Zr as the LUMO, as well as π_{CC} and σ_{CC} of the C = C bond, and the two Zr – O bonds as filled levels. It is obvious from Figure 1, that a synchronous "least motion" in-plane coupling of the two acetyl ligands, maintaining C_{2v} symmetry, is a strictly forbidden reaction and therefore should have a high energy barrier. The situation is quite analogous to that reported by us earlier[9] for bis-acyl actinide complexes. There, however, bis-acyl compounds, formed by double CO insertion, are isolable intermediates in some cases. Intramolecular coupling of two metal-coordinated acyl groups (*both* η^2 in the minimum energy structure) can occur and is energetically accessible, if the metal-centered rearrangement, which takes the bis-acyl ligand set to the enediolate structure, involves a conrotatory motion of both COR groups along the coupling itinerary. From Figure 1 it is easy to derive the qualitative consequences of allowing related low-symmetry coupling path-

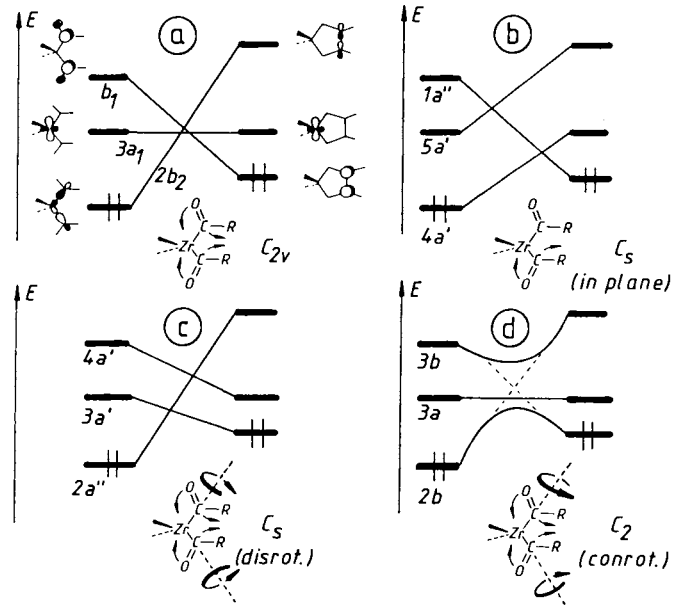

Figure 2. Comparison of frontier level correlations for the bis-acyl complex (η^1-η^1) to enediolate complex transformation along the a) C_{2v} least motion pathway; b) C_s (in-plane) pathway; c) C_s (disrotatory) pathway; d) C_2 (conrotatory) pathway

ways for our Zr model system as well. We only need to focus upon the three relevant frontier orbitals labeled b_1 (π^*_{CO} + π^*_{CO}), $3a_1$ ("y^2"), and $2b_2$ (σ_{Zr-C} − σ_{Zr-C}) in Figure 1 on the starting compound side, which correlate to π_{CC}, "y^2", and σ^*_{CC} of the enediolate product. As seen from Figures 2b and 2c in comparison to 2a (the C_{2v} coupling), neither any less symmetrical ("nonsynchronous") in-plane motion (C_s, in-plane) of both acetyl groups nor their disrotatory out-of-plane movement (C_s, disrotatory) along the coupling path can help to circumvent the symmetry-forbidden course of enediolate formation. Only if we allow for a conrotation of the acyl groups during oxygen to Zr coordination and C−C fusion, lowering the maximum symmetry of the process from C_{2v} to C_2, the fatal orbital crossing would be eliminated (Figure 2d). Still, however, as indicated in Figure 2d, an avoided crossing of levels will remain and will probably impose on appreciable barrier upon acyl coupling, despite its formally allowed course.

We have calculated a two-dimensional energy surface for the intramolecular acyl coupling to assess, at least semi-quantitatively, the energetic requirements for C_{2v} vs. C_2 (conrotatory) acetyl coupling pathways in our model system $Cp_2Zr(COCH_3)_2$. The computations started from structure **16** in Scheme 6 with both acetyl groups η^2-coordinated. As detailed above, this geometry lies already 29.4 kcal/mol above the best η^1-η^2 ground state isomer **12**, 27.1 kcal/mol above the η^1-η^2 isomer **13** with both oxygens "O-outside", and 23 kcal/mol above the corresponding η^1-η^1 structure **17**. As the enediolate formation necessarily encompasses oxygen to Zr coordination along the reaction pathway, and as the energy of **16**, relative to its other isomers of Scheme 6, was known, we considered **16** as a reasonable starting point for checking computationally the energetics for the acyl coupling process[22]. The energy surface shown in Figure 3 was then computed according to Scheme 7.

Scheme 7

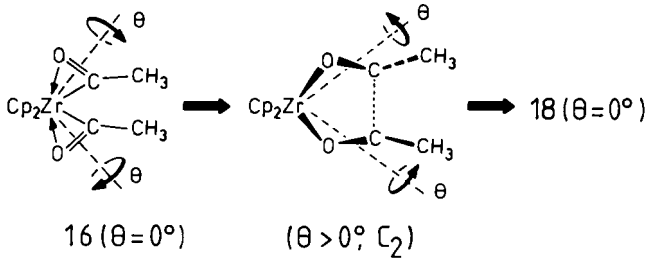

The conrotation of both acetyl groups was modeled by varying the angle of rotation around the vectors pointing from Zr to the midpoints of the two C−O bonds. The reaction pathway Δr_i from **16** to **18** was a simultaneous change of all those bond distances and bond angles, that alter their respective values along the ligand set transformation (Cp_2Zr fragment kept fixed). The total variation for each distance and angle between **16** and **18** (e.g. C−C going from 368.5 pm in **16** to 131.5 pm in **18**, Zr−C from 219.7 pm in **16** to 285.7 pm in **18**, C−O from 121 pm in **16** to 136.9 pm in **18** etc.) was dissected into ten equidistant intervals, thus simultaneously changing all parameters. Certainly, this is a crude simplification of the true minimum energy pathway, but it is giving valuable insights. The results are displayed in Figure 3.

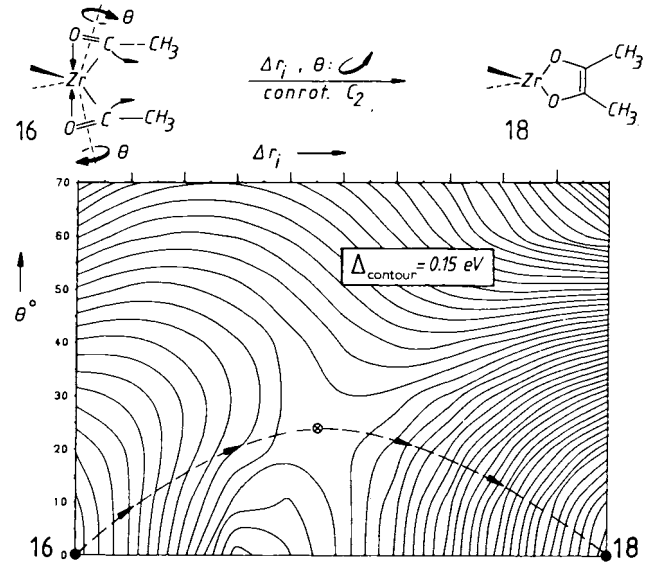

Figure 3. Computed two-dimensional energy surface for the **16** to **18** transformation. The dotted line represents the symmetry allowed conrotatory C_2 pathway with its transition state at the crossed circle. The transit along $\Theta = 0°$ is the symmetry forbidden C_{2v} path. The 10-step reaction coordinate Δr_i on the abscissa is described in the text

The minimum energy reaction path (broken line) leading from **16** to **18** as expected involves rotation of both acyl groups until a value of $\Theta = 25°$ is reached at the transition state (crossed circle). Then Θ goes back to 0°, until the planar enediolate structure is finally formed. The energetically less favorable transit from **16** to **18** without conrotation ($\Theta = 0°$ throughout) corresponds to the C_{2v} symmetry-forbidden path of Figure 1. The calculated barrier between **16** and the transition state is around 1.8 eV (42 kcal/mol), the rearrangement process as a whole is highly exothermic (**18** being 2.25 eV = 52 kcal/mol more stable than **16**). If we additionally take the fact into consideration, that our η^2-η^2 starting geometry **16** itself is already around 25−30 kcal/mol higher in energy than any of the η^1-η^2 structures or an η^1-η^1 geometry (viz. Scheme 6), we must conclude that even a formally symmetry-allowed conrotatory ligand coupling along the proposed bis-acyl path of Scheme 3 is energetically not feasible, although the rearrangement from the best η^1-η^2 structure **12** of $Cp_2Zr(COCH_3)_2$ to the enediolate is still exothermic by approximately 22 kcal/mol[23a], in accord with the experimental irreversibility of the reaction. The prohibitively high barrier[23b] calculated for a bis-acetyl coupling at Cp_2Zr strongly contrasts the rather small computed barrier of the analogous process for actinide compounds (ca. 16 kcal/mol)[9]. The difference between the two seemingly related systems does not only stem from the fact the actinide bis-acyl systems prefer η^2-η^2 ground-state structures, whereas bis-cyclopentadienyl group 4 derivatives tend to

follow the EAN rule and bind the two acyl groups in a mixed η^1-η^2 fashion. As we have seen from Figure 3, even starting out from the enforced $Cp_2Zr(\eta^2\text{-}COCH_3)_2$ structure **16** leads to a calculated barrier towards intramolecular acyl coupling, which is by far exceeding that for $Cp_2Th(\eta^2\text{-}COCH_3)_2$ or $Cp_2U(\eta^2\text{-}COCH_3)_2^{2+}$. From our analysis of the transition state of Figure 3 we conclude that its high energy is predominantly due to its bis-zirconoxycarbene character. We have shown previously[11b] that zirconoxycarbene isomers **19** of η^2- or η^1-acyl complexes are generally high-energy species, **19** being around 2 eV above its η^2-$COCH_3$ isomer.

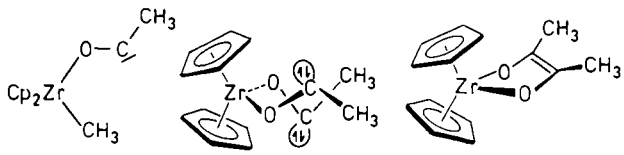

19 20 21

Even if a ligand coupling process for, e.g., $Cp_2Zr(COCH_3)_2$ does not necessarily have to proceed along a truely synchronous conrotatory C_2 coupling pathway, the simplified rearrangement itinerary of Figure 3 should contain the essence of the necessary ligand motions and inevitably leads through transition points similar to the geometry displayed in **20**, where the Zr–O bonds are already formed but no carbon–carbon bond has evolved yet. For actinide metals their larger atomic size allows much better to avoid the pronounced development of oxycarbene character along the "concerted" acyl coupling pathway, because carbon to metal interactions can be maintained until the two acyl carbons begin to form the new C=C bond. The combined requirements of having to avoid a 20-electron configuration (avoiding two η^2-acetyl groups at any point) and of circumventing a symmetry-forbidden course (by conrotatory out-of-plane motions), forces intermediate structures with pronounced zirconoxycarbene character to appear on the bis-acyl-coupling pathway. They are responsible for the computed prohibitive barriers.

It should be mentioned that the planar C_{2v} enediolate ring geometry implied so far is not the true minimum structure of such molecules. Theory as well as X-ray structure investigations have told us[24] that enediolate rings are not planar, but folded around the O–O axis as shown in **21**. Their barrier to inversion is very small, and we need not worry about this electronically interesting distortion, which is directly related to the deep color of monomeric Cp_2Zr- and Cp^*_2Zr-enediolates and related compounds. It does not change any of our conclusions.

To summarize at this point: according to the model MO calculations a concerted direct coupling of two Zr-bound acyl groups, following a double carbonylation of bis-organyl precursors Cp_2ZrR_2 or $Cp^*_2ZrR_2$ as implied in Scheme 3 and as tentatively suggested in the literature, does not appear to be a viable pathway for enediolate formation. Other mechanisms have to be considered and tested.

The η^2-Ketone Pathway

When alternative reaction channels for enediolate formation are sought, it is the electronic structure of monoacyl species (**5**–**7**), which, in connection to several experimental findings, may provide relevant information. As shown in Scheme 2 for the **5** to **7** interconversion, oxygen decoordination and rotation of an η^1-acyl group is easily achieved in monocarbonylation products $Cp_2Zr(COR)(R)$. While in $Cp_2Zr(\eta^2\text{-}COR)(R)$ the LUMO, namely the low-lying[25] π^*_{CO} orbital of the η^2-acyl group, is oriented orthogonally to the high-lying Zr–R σ-bonding orbital, as depicted in **22** (η^2, "O-outside") and **24** (η^2, "O-inside"), oxygen decoordination and η^1-acyl rotation lead to a situation, where, as shown in **23** for a fully upright η^1-acyl group, the π^*_{CO} orbital with its dominant carbon p-contribution and the Zr–R σ-bond are in the same plane. In localized orbital terms, a "carbanionic" group R has its high-lying carbon to metal-bonding electron

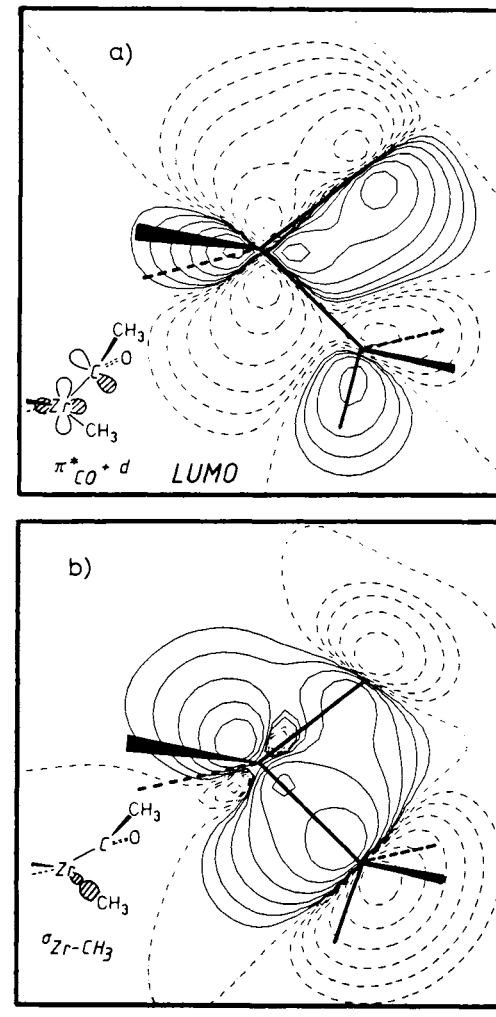

Figure 4. a) LUMO for $Cp_2Zr(\eta^1\text{-}COCH_3)(CH_3)$ with an upright acetyl group, composed of π^*_{CO} and in-plane metal d-AO contributions, plotted within the C–Zr–C plane; b) high lying Zr–C_{CH_3} bonding MO of $Cp_2Zr(\eta^1\text{-}COCH_3)(CH_3)$ with a perpendicular acetyl group, plotted in the same plane. The solid (dashed) lines correspond to positive (negative) values of +/−0.4, +/−0.2, +/−0.1, +/−0.05, +/−0.025, +/−0.0125, +/−0.005 for the wavefunctions, zero contours are also shown

pair geometrically fixed on the backside of, in the same plane as, and in close proximity to the carbon p-orbital lobe of a carbonyl group π^*_{CO} orbital. This is precisely a geometric requirement for the minimum energy approach of a nucleophile attacking a carbonyl group (viz. **25**)[26].

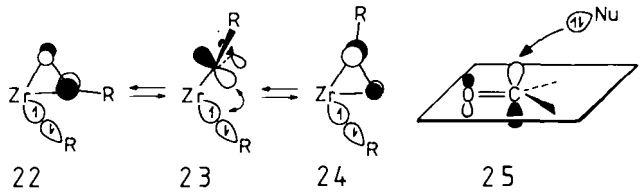

22 23 24 25

An elcctronic situation as in **23**, locating both groups in a mutual *cis*-geometry due to the bent sandwich metal template, strongly suggest the possibility of facile carbon–carbon bond formation by R to COR migration. Figure 4 gives contour diagrams of the LUMO as well as of the high-lying $Zr-C_{CH_3}$ σ-orbital, as they evolve from MO calculations for $Cp_2Zr(\eta^1\text{-}COCH_3)(CH_3)$ with an upright acetyl group. Note that Figures 4a and 4b display two different canonical MOs; in **23** their localized equivalents have been shown within the same picture for simplicity. The LUMO in Figure 4a is notably delocalized onto the Zr atom. It is really the in-phase combination of π^*_{CO} with the y^2 d-AO at the metal und therefore lies even lower than an acetyl π^*_{CO} MO.

Of course less pronounced out-of-plane distortions than a 90°-rotated conformation **23** could suffice to induce the type of R to COR interaction discussed here. It is only the strictly in-plane η^2 coordination mode (**22**, **24**) that allows no overlap between the two wave functions in question.

Experimental evidence for intramolecular R to COR bond formation in monoacyl complexes is available. Erker has shown[27a] that according to Scheme 8 $Cp_2Zr(\eta^2\text{-}COPh)(Ph)$ (**26**) and related aroyl aryl systems can be converted to dimeric η^2-benzophenone complexes **27**.

Scheme 8

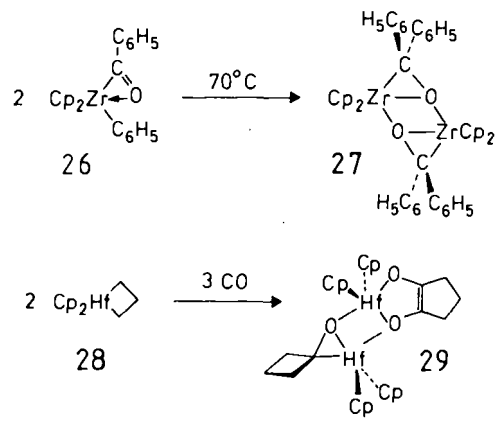

Apparently, a phenyl group migration to the benzoyl carbon and oxygen coordination generate η^2-benzophenone as a ligand; two monomeric "zirconaoxirane" species then dimerize to **27**. Similar carbon–carbon coupling within the coordination sphere of CpCp*Zr, forming an η^2-acylsilane ligand $(CH_3)CO[Si(SiMe_3)_3]$ has been postulated recently[27b], and η^2-ketones from acyl-alkyl coupling steps also seem to occur for Cp*MCl (*s-cis*-diene) complexes (M = Ti, Zr, Hf)[27c]. We also remind the reader that Floriani's synthesis of **10** in Scheme 4 is an intermolecular version of η^2-aldehyde formation from a (postulated) acyl complex. Moreover it has been reported that carbonylation of the hafnacyclobutane **28** directly yields **29**[28], a 1:1 adduct of an η^2-cyclobutanone complex of Cp_2Hf with the corresponding enediolate. The enediolate product – once formed – seems to trap its η^2-ketone precursor. Obviously, the latter reaction is closely related to Grubb's transformation from **3** to **4** of Scheme 1. Although it has not been possible to carbonylate **27** or **29** further and to get enediolate complexes as final products, the formation of **27** and **29** and our electronic structure description for $Cp_2Zr(\eta^1\text{-}COCH_3)(CH_3)$ (viz. **23**) point to the general pathway of intramolecular enediolate production shown in Scheme 9 for our $Cp_2Zr(CH_3)_2$ model.

Scheme 9

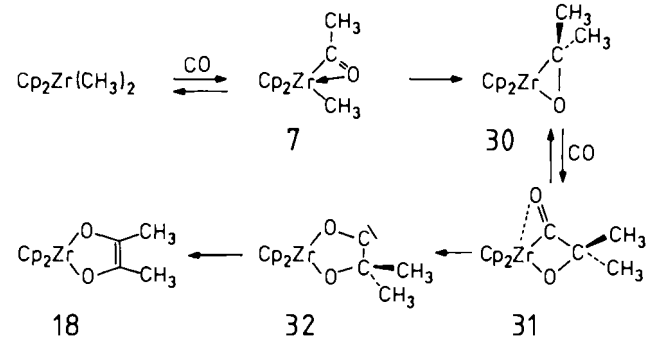

The central point of this scheme is the η^2-acetone complex **30**, which can be viewed as a zirconaoxirane in an alternative resonance description. Carbonylation of such a species could lead to **18** via **31** and **32**. The latter two need not be true intermediates; the rearrangement of a CO-inserted zirconaoxirane **31** and the 1,2-alkyl shift could go simultaneously. Structure **32** is only shown to make clear the overall process. In the following we will describe results of MO model calculations for the conversion of **7** to **30**, as this is the step which has to be compared first to the energetic situation described for bis-acyl coupling in the previous section. Let us begin with the η^2-acetone complex **30**, the endpoint of the step we want to study. Monomeric η^2-ketone and η^2-aldehyde complexes are known for various metals. In **30** formally a d^2 fragment, Cp_2Zr, binds to the organic moiety, which leaves **30** with 2 electrons less than the stable molecule $Cp_2Mo(\eta^2\text{-}CH_2{=}O)$[29]. In Figure 5 (above) a simplified interaction diagram is given for $Cp_2Zr(\eta^2\text{-acetone})$ (C_s), showing the familiar levels of a C_{2v}-d^2-Cp_2Zr fragment[21] interacting with the relevant levels of the acetone ligand. An off-axis location of the organic ligand's C–O bond within the molecular plane of symmetry ("O-inside") corresponds to the minimum energy structure, if the η^2-acetone position is optimized[30].

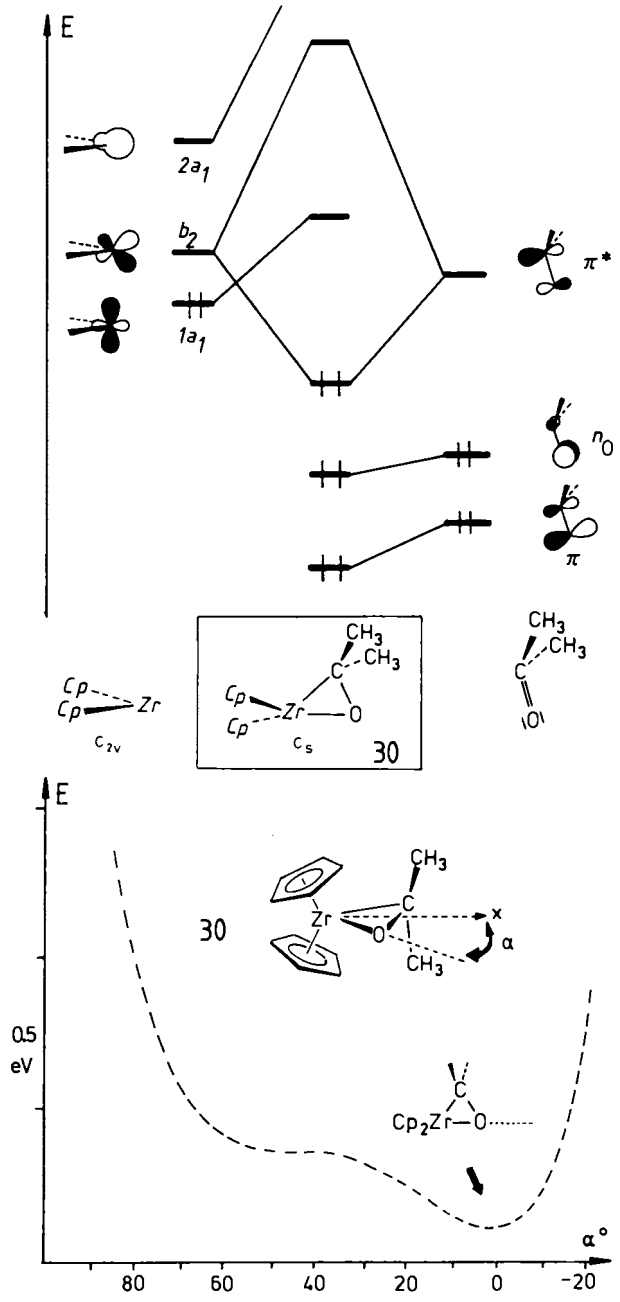

Figure 5. Above: Simplified interaction diagram for **30** between a Cp_2Zr unit (d^2) and an η^2-acetone ligand for the minimum energy location of the organic moiety. Below: Total energy curve for moving an η^2-bound acetone unit within the molecular plane of symmetry of $Cp_2Zr(\eta^2$-acetone). The location of the CH_3-C-CH_3 plane is optimized with respect to its bending-back angle. α is the *x*-axis-Zr−O angle

As seen from Figure 5 (below) an in-plane pivoting motion of the η^2-ketone causes a very shallow energy profile for rather large deviations away from a "central" coordination mode (α around 20°). The reason for this soft potential curve is obvious: the Cp_2Zr fragment MOs $1a_1$ and b_2 provide practically equivalent π-backbonding to π* of the CO group for a central as well as for an off-axis location of the C−O midpoint. It is the low-lying LUMO of $Cp_2Zr(\eta^2$-acetone) in Figure 5 (above), a metal-localized orbital displayed in Figure 6a, which is responsible for the instability of monomeric η^2-ketone, -aldehyde, -ketene, or similar η^2-CO-bound d^2-Cp_2M complexes. It causes their dimerization by Zr−O linkages if this is sterically possible or, most important to our further discussion, it leads to attachement of an auxiliary two-electron donor ligand.

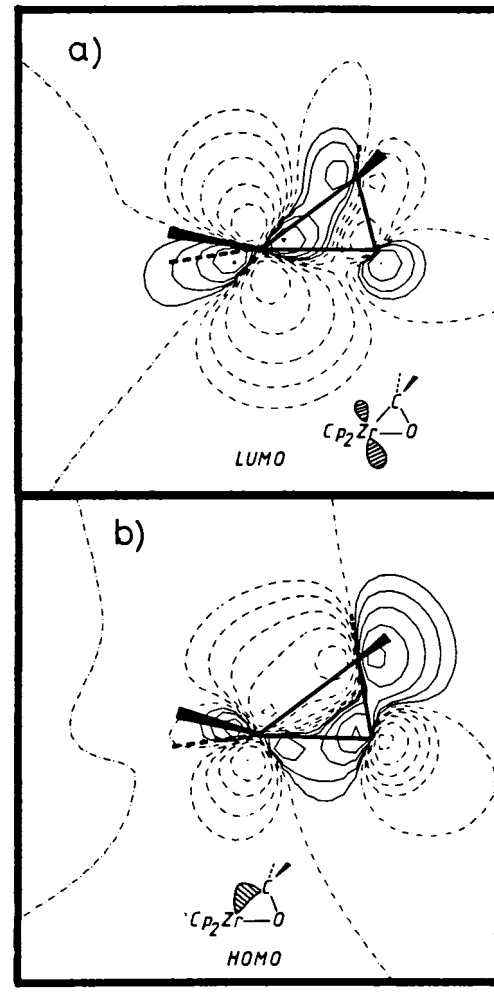

Figure 6. Contour plots for a) LUMO and b) HOMO of $Cp_2Zr(\eta^2$-acetone) (**30**) within the plane of the zirconaoxirane ring. Contour values as in Figure 4

The highest occupied MO of zirconaoxirane **30** is shown in Figure 6b, it is largely localized in the Zr−C bond of the three-membered ring and represents a typical "bent bond" of a strained Zr−C−O ring system with a nucleophilic carbon atom. With respect to Scheme 9, the intermediate **30** could offer the necessary prerequisite for a consecutive carbonylation: a low-lying LUMO to induce CO attack by CO lone pair coordination as well as an energetically high-lying, strained Zr−C orbital to interact efficiently with an empty π^*_{CO} orbital, facilitating insertion. Thus the electronic structure of **30** would support the mechanism of Scheme 9, *provided that the* **7** *to* **30** *rearrangement is facile enough.* It seemed therefore essential to take a closer look at this methyl to acetyl transfer step. This was done in model calculations, which started out from $Cp_2Zr(\eta^1$-$COCH_3)(CH_3)$ with an upright η^1-$COCH_3$ group as in **23** to ensure optimal

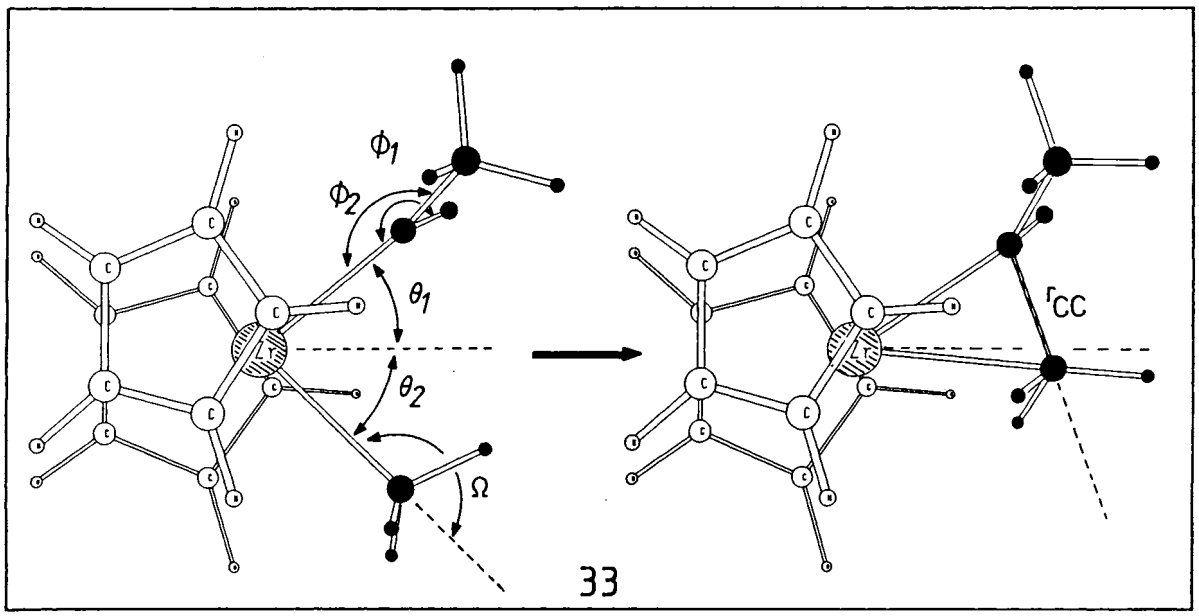

interaction between the $Zr-CH_3$ bond and π^*_{CO} of the acetyl ligand from the beginning. To get a detailed insight into the electronic structure variations along the transit from **7** to **30**, and because a computation of the complete energy-minimized reaction pathway with full geometry optimization is unreasonable within the framework of EH theory, we modeled the complicated overall molecular geometry change between $Cp_2Zr(\eta^1\text{-}COCH_3)(CH_3)$ (**23**, acetyl upright) and the η^2-acetone complex **30** as two separate processes. We first calculated the initial $C_{CH_3}-C_{COCH_3}$ coupling step to get an estimate of the energetics associated with the onset of the methyl to acetyl group transfer indicated in **23** above. Based upon the qualitative considerations (vide supra) a low barrier or even a gain in energy could be expected.

As shown in **33**, we mimicked the initial phases of the CH_3-COCH_3 bond formation by independently optimizing angles Θ_1 and Θ_2 (their sum determines the $C_{CH_3}-C_{COCH_3}$ distance r_{CC}), Φ_1 and Φ_2 (allowing for pyramidalization at the carbonyl carbon in the course of the methyl group's approach), and Ω (reorienting the methyl group's C_3 axis towards its new bonding partner). All other geometric parameters were kept fixed during this first set of calculations. Their results are presented in Figure 7. Unexpectedly, varying all geometric parameters of **33** independently over a wide range inevitably causes the energy to increase! Figure 7a displays the change in total energy corresponding to the *lowest energy* pathway, when we enforce an approach of the CH_3 group to the acyl carbonyl center.

The points plotted along this least energy curve of Figure 7a represent six geometries of the "reacting system" $Cp_2Zr(\eta^1\text{-}COCH_3)(CH_3)$ with their $C_{CH_3}-C_{COCH_3}$ distances varying between 306 (= **I**) and 156 pm (= **VI**) and with their corresponding optimal angular variables Θ_1, Θ_2, Φ_1, Φ_2, and Ω also given below the diagram. Plots of the structures for these geometries **I**–**VI** are shown in Figure 7b. While the carbon–carbon distance decreases from 306 to finally 156 pm by predominantly methyl group migration towards $COCH_3$, and while the new C–C bond is formed, accompanied by appropriate acyl group pyramidalization and CH_3 group reorientation towards the carbonyl C atom, the energy goes up by around 1.5 eV (ca. 35 kcal/mol), in contrast to our expectation of a facile ("Grignard-type") nucleophilic attack at the carbonyl group. The unfavorable picture does not change, even if at later stages of the CH_3 transfer (e.g. for **IV**, **V** and **VI**[31]) the migrating methyl group is allowed to move further away from Zr within the

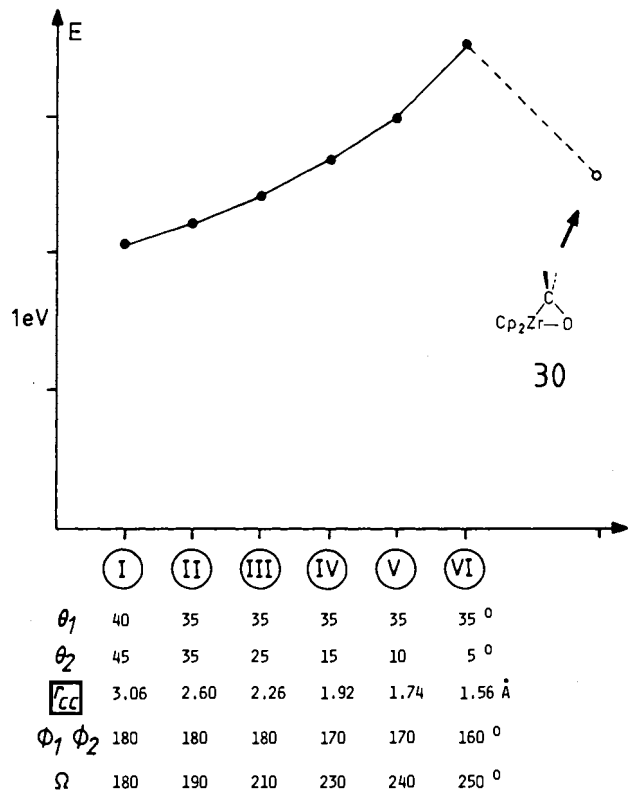

Figure 7a). Total energy variation along waypoints **I**–**VI**, representing the initial CH_3-COCH_3 coupling process of least energy ascent. The total energy of the η^2-acetone complex is included for comparison

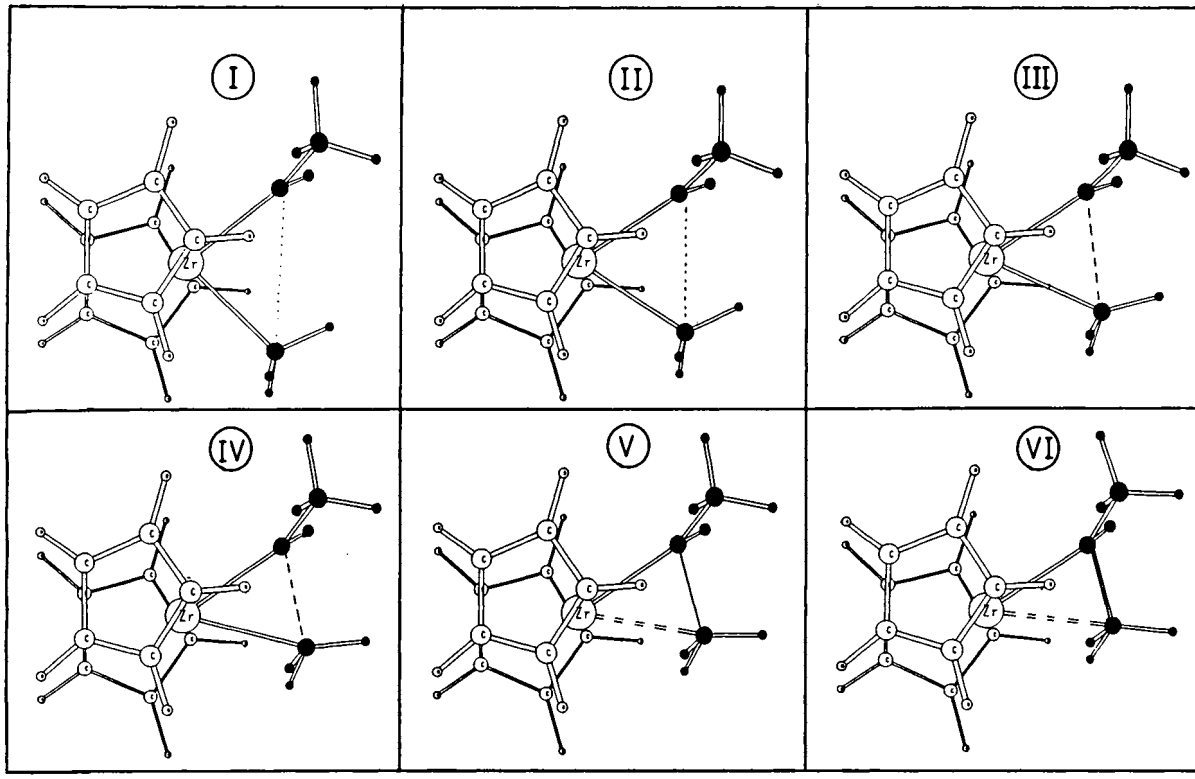

Figure 7b). Geometries **I**–**VI** corresponding to the total energy curve of Figure 7a). "Reacting" ligand set atoms are shaded

Zr–C–C plane (i.e., if the Zr–C_{CO}–C_{CH_3} angle is additionally optimized). As depicted in **34**, we also allowed for a simultaneous rotation (angle τ) around the Zr–C_O bond of the new $C(O)(CH_3)_2$ unit, while independently optimizing the positions of its oxygen and its CH_3 groups (arrows in **34**).

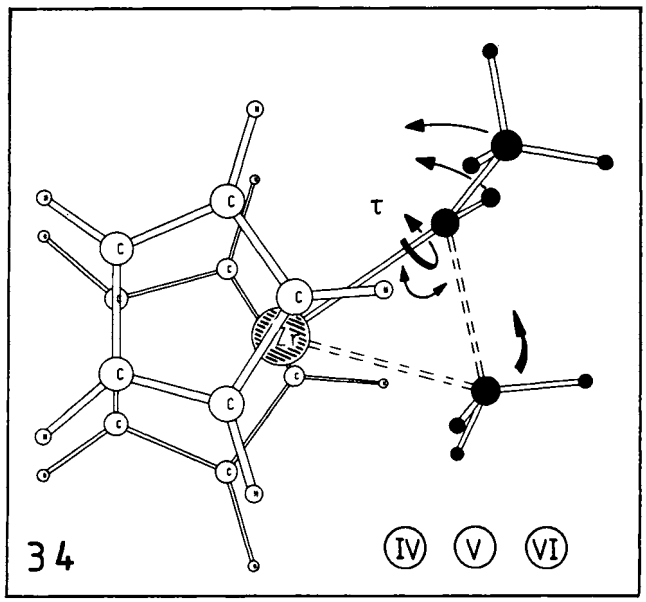

These additional degrees of freedom in **34** open relaxation modes towards the final η^2-acetone complex **30** by coordinating the former acyl oxygen center to Zr and rotating the migrated CH_3 out of plane. Interestingly, neither **IV** nor **V** and **VI** show any tendency to relax structurally along those channels. Conversely, starting out from, e.g., **IV**, which is itself around 0.65 eV (ca. 15 kcal/mol) above **I**, an additional barrier of about 1.4 eV (32 kcal/mol) has to be overcome to finally reach the acetone complex **30**. The situation is worse for **V** and **VI**. Even if we take again into account that our model calculations, as in the bis-acetyl coupling investigation above, only may give an upper energy limit due to their restricted nature, the overall result at first glance seems to rule out the pathway proposed in Scheme 9.

At this point a thorough inspection of the orbitals of the $Cp_2Zr(COCH_3)(CH_3)$ model and of their behavior along the reaction coordinate of our "enforced" methyl transfer reaction process not only reveals the origin of its high energy demands, but also suggest a mechanistic variant of Scheme 9, which allows to avoid prohibitive activation barriers.

The Electron Donor Supported (CO-Induced) η^2-Ketone Pathway

An orbital correlation diagram for the methyl transfer process (**I** to **VI**) in $Cp_2Zr(COCH_3)(CH_3)$ shows the expected smooth conversion of the Zr–CH_3 bonding orbital (viz. Figure 4b) to the MO of the newly formed methyl to acetyl C–C bond. This transformation of a bonding pair with Zr–C σ-type is a stabilizing contribution to the total energy change. A more relevant observation, however, concerns the behavior of the LUMO wavefunction along the gradual transit from **I** to **VI**. Figure 8 plots the lowest unoccupied MO for all six points of Figure 7.

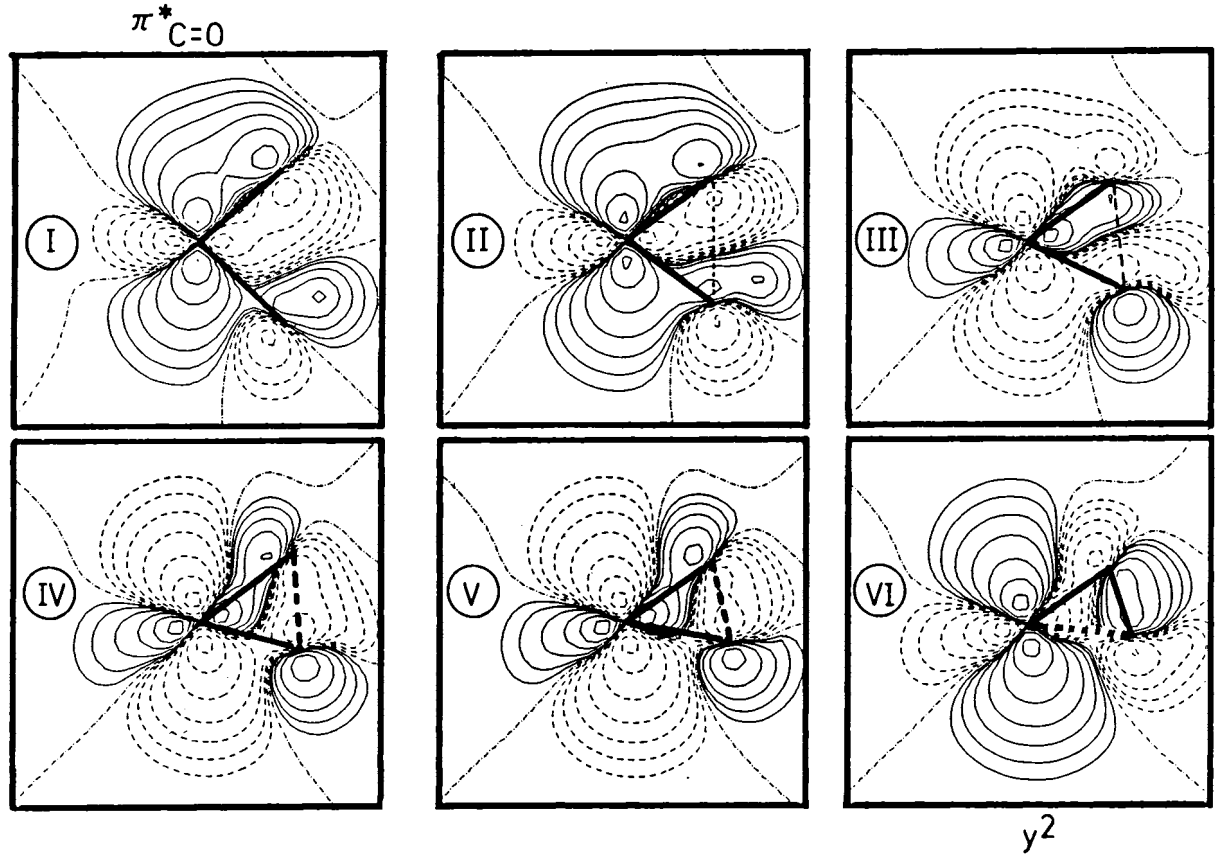

Figure 8. Evolution of the LUMO wavefunction along the methyl group transfer path of Figure 7. The plots correspond to geometries **I** to **VI** (Figure 7b), the contour values are as in previous figures. Only the two in-plane Zr–C bonds to the methyl and acetyl carbons as well as the newly formed C–C connectivity are indicated

Going from **I** to **VI** the LUMO changes its orbital character dramatically. Being of mainly π^*_{CO} character within the acetyl ligand at the starting point **I** (viz. also Figure 4a), it adopts more and more metal d character, finally becoming a heavily zirconium-localized ("y^{2}") d orbital in **VI**. It is easy to see, how this transformation occurs, and we can explain it by help of the qualitative correlation diagram of Figure 9, in which only those levels are shown, which participate directly in the methyl transfer to the acyl carbon.

Apart from the occupied σ_{Zr-CH_3} MO in Figure 9, three empty levels of $Cp_2Zr(\eta^1\text{-}COCH_3)(CH_3)$ (**23**) are important, namely the LUMO π^*_{CO} with its in-phase contribution from y^2 at Zr, the next level above the LUMO, which is the y^2 orbital at Zr (with antibonding admixture from π^*_{CO}) and, at higher energy, the antibonding $\sigma^*_{Zr-CH_3}$ MO. When the CH_3 group couples to the acyl carbon along the pathway of Figure 7b, the π^*_{CO} LUMO, interacting with the migrating CH_3 electron pair, is strongly destabilized and wants to correlate with the new antibonding σ^*_{C-C} orbital of geometry **VI**. The metal d orbital y^2 of course intends to correlate with the equivalent[32] y^2 of the product, and $\sigma^*_{Zr-CH_3}$ on the starting compound side wants to transform into an empty acceptor d orbital of σ-type[32] of **VI**, which points towards the position vacated by the methyl shift. For symmetry reasons (all MOs shown in Figure 9 are of the same symmetry) the intended correlations (dotted lines) lead to the actual MO correlation picture of Figure 9 (solid lines). The resulting

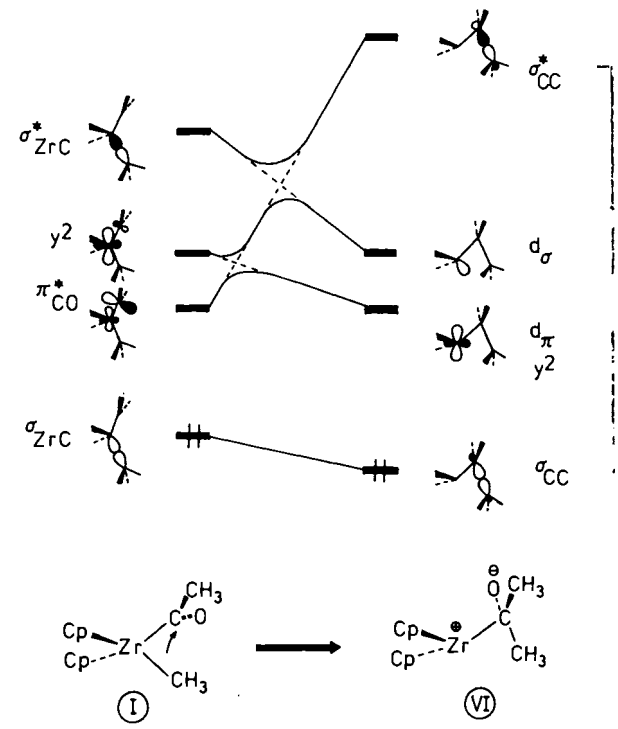

Figure 9. Qualitative MO correlation diagram for the methyl to acetyl transfer process of Figure 7. Only the levels discussed in the text are shown

relation between the LUMOs on both sides is the origin of the smooth transformation of π^*_{CO} into y^2 along the CH_3 transfer path as shown in Figure 8 above. The overall process of forming the C–C bond between the methyl carbon and the acyl carbon is energetically uphill, because the favorable replacement of a $Zr-CH_3$ by a C–C bond is outweighted by accompanying repulsive interactions between the migrating CH_3 group's electron pair and the $Zr-COCH_3$ σ-bonding pair. In essence, the **I** to **VI** transit with the methyl group undergoing its formal anionic 1,2-shift from Zr to the acyl carbon leads from a 16-electron complex of the Cp_2ZrR_2-type to a 14-electron system. It is this 14-electron situation, which is reflected in the evolution of the *two* low-lying empty metal levels of Figure 9 and causes the unexpectedly high barrier for methyl-acyl coupling in Figure 7a. This barrier has to be overcome before oxygen attachment to Zr and concomitant $CO(CH_3)_2$ fragment relaxation can produce the η^2-acetone complex, which itself is electron-deficient and higher in energy than the $Cp_2Zr(\eta^1\text{-}COCH_3)(CH_3)$ starting point.

There is an obvious conclusion, that can be drawn from this analysis: methyl to acetyl coupling should be facilitated and may perhaps become a low-energy process, if the electron demand developing at the metal during the CH_3 shift is simultaneously satisfied, i.e. if the electron pair "lost" into the new C–C bond by methyl shift is simultaneously replaced by a new electron pair from somewhere else. In MO terms, methyl to acyl coupling should be supported or should even be induced by appropriate nucleophiles interacting as 2-electron donors with the metal-centered LUMO, which successively grows at the metal as the CH_3 group begins its interaction with the π^*_{CO} orbital of the acetyl group. We have tested this conclusion computationally by simply taking a CO molecule as an external nucleophile. As depicted in **35**, we recalculated all six geometry points **I**–**VI** of Figure 7 (parameters Θ_1, Θ_2, Φ_1, Φ_2, Ω, r_{CC} as above), adding a CO molecule at a fixed Zr–CO distance of 250 pm within the plane of the CH_3 shift. The relative angular CO position was independently optimized for each waypoint **I**–**VI**[33], leading to a preferred location on the side of the migrating methyl group (bottom side in **35**) from point **II** onwards.

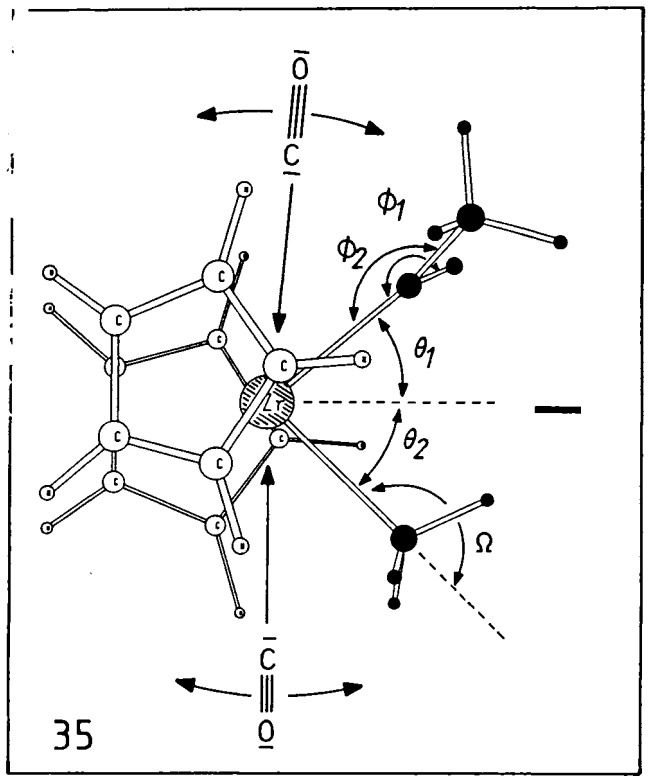

In Figure 10 the resulting energy profile is shown (filled squares) in comparison to the one obtained earlier (Figure 7a) without CO participation, which is included for comparison (filled circles). Both η^2-acetone complexes with and without CO (**30**) are also given.

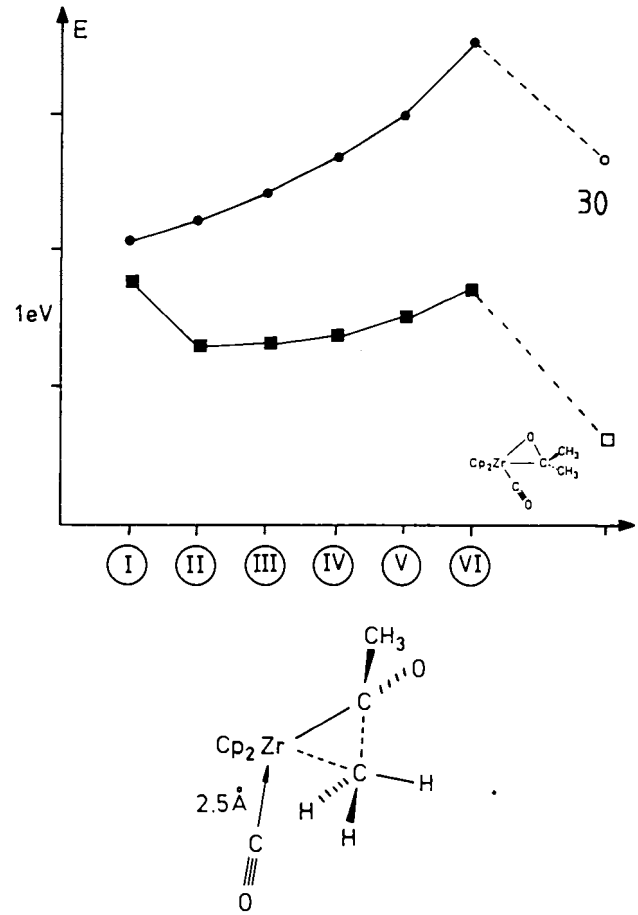

Figure 10. Total energy profile (filled squares) for a methyl to acetyl shift along the **I** to **VI** model pathway of Figure 7 in the presence of a CO molecule 250 pm apart from the Zr center, with its angular position on the CH_3 side optimized independently. The earlier curve (without CO participation) of Figure 7a is included for direct comparison (filled circles). The total energy for both η^2-acetone complexes (with and without CO) is also given. The geometry parameters of **I**–**VI** are as in Figure 7

For the starting geometry **I**, $(Cp_2Zr(\eta^1\text{-}COCH_3)(CH_3)$, acetyl group upright), the presence of CO causes a minor stabilization. Its magnitude (ΔE between both curves) increases while the methyl transit takes place through **II** to **VI**, indicating the growing electron demand at Zr along the

model reaction coordinate. The downhill slope between **I** and **II** indicates a nucleophile-driven C–C coupling to occur. The energy ascent from **II** to **VI**, where the new C–C bond is practically formed, is reduced to less than 9.2 kcal/mol, the CO-coordinated acetone complex is 37 kcal/mol lower in energy than **I** + CO. Moreover, if we recompute the ligand relaxation leading to an η^2-type acetone coordination mode as shown and described by **34** for the stages **IV** – **VI**, but now in the presence of the external CO, we find it to be a favorable process. For geometry **IV** this is displayed in Figure 11, which compares the change in energy for the rotational ligand relaxation of **34** without CO attack (upper curve, open circles in Figure 11) to the energetics of the same process with CO (CO 250 pm away, angular position optimized, lower curve, filled circles). Even at stage **IV**, where the CH_3 transfer to the $COCH_3$ group is not complete and the $C_{CH_3}-C_{COCH_3}$ distance is still 192 pm, the incoming CO reduces the barrier necessary for going to $\tau = 50°$ to about 10 kcal/mol. Along with the rotation the acyl oxygen moves towards Zr. When we optimize all degrees of freedom indicated by arrows in Figure 11 for geometry **IV** at the fixed $C_{CH_3}-C_{COCH_3}$ distance of 192 pm, then the lower curve in Figure 11 respresents the practically complete rotational relaxation towards a still somewhat distorted, CO-coordinated η^2-acetone complex. In comparison to the profile for **IV** without CO it starts out at lower energy for the upright structure ($\tau = 0°$) and shows a different ligand set arrangement (the $CH_3/COCH_3$ ligand couple adapts to the needs of the attacking CO at $\tau = 0°$) already before rotation and relaxation towards the η^2-acetone structure begin.

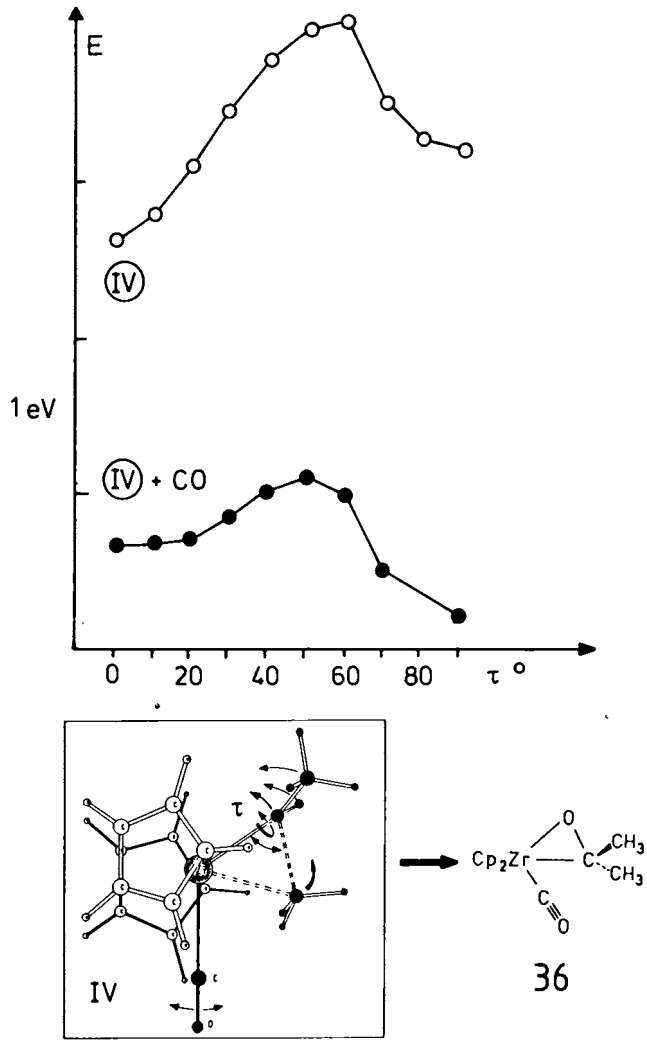

Figure 11. Total energy curves for relaxing geometry **IV** of Figures 7 and 10 (r_{CC} = 192 pm) towards the η^2-acetone geometry as described by **34**. Upper curve: no CO present. Filled circles: **IV** with CO at 250 pm distance, CO angular position optimized. τ is the rotation angle around the $Zr-C(O)(CH_3)_2$ bond, $\tau = 0°$ correponds to the shifting methyl group still in the mirror plane of the Cp_2Zr moiety; for details see text

Combining the results of Figures 7, 10, and 11 we can conclude that the anticipated η^2-ketone formation of Scheme 9, essential for the mechanism of enediolate formation postulated above, is a low-energy pathway, if the shift of the Zr-bound alkyl group to the electrophilic acyl carbon is assisted by an additional incoming ligand. We therefore think that Scheme 9 has to be modified accordingly. If CO participates in the ketone-producing step directly, then we should of course expect an intermediate $Cp_2Zr(\eta^2\text{-acetone})(CO)$ complex **36** as shown in Scheme 10 instead of an unligated η^2-acetone complex **30** of Scheme 9.

Scheme 10

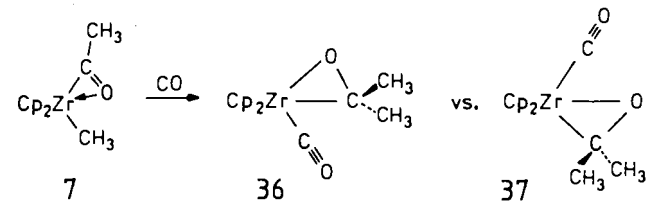

This mechanistic picture suggests that stereoisomer **36** should be the primary product of a CO-assisted η^2-ketone formation. In comparative calculations for the respective groundstate geometries of **36** and **37** (taking Zr–CO = 200 pm and optimizing the ligand group positions) the isomeric carbonyl complex **37** is found to lie around 8 kcal/mol higher in energy. From **36** onwards Scheme 9 should apply: CO insertion and rearrangement through **31** and **32** lead to **18**. We have not calculated the detailed reaction path from **36** onwards, and therefore our calculations, although they predict **36** as a reaction intermediate, do not allow us to draw a conclusion as to its actual barrier towards insertion and rearrangement to **18**. Some qualitative statements, based on structure and electronics, can be made however. We may expect that inserting CO into the Zr–C bond of the zirconaoxirane ring of **36**, our predicted key intermediate, should be thermodynamically less favourable, i.e. might also possess a higher kinetic barrier than the initial CO insertion into a $Zr-CH_3$ bond of $Cp_2Zr(CH_3)_2$, because the potential insertion product **31** is less capable of adopting the stabilizing η^2 coordination mode of the newly formed acyl group on geometric grounds. Thus, a higher product instability of **31** may counteract the above mentioned good backbonding interaction between the high-lying zircona-

oxirane (Walsh-type) Zr–C "bent bond" σ-orbital (Figure 6b) and a π* MO of CO, which itself would favour insertion and Zr–C bond breaking. It is hard to estimate which tendency will dominate the barrier of the insertion step. We note in this context that Norton et al. have reported CO insertion into an η^2-bound binuclear Zr-acetone complex very recently[18d]. Their isolated product is closely related to structure **32**, stabilized and "trapped" by two Cp_2ZrX fragments. Structures of type **31**, if formed once, should easily rearrange to their enediolate isomers (e.g. **18**) on thermodynamic and kinetic grounds. Both transformations, from **31** to **32** as well as from **32** to **18**, if considered separately, are expected to be symmetry-allowed and to go energetically downhill. It is highly probable that they would occur simultaneously, because oxygen to Zr coordination (even before complete $Zr-C_{acyl}$ bond rupture) creates an electronic situation equivalent to that inducing 1,2-shifts of R groups in carbenium ions, because η^2-acyl groups intrinsically have carbenium ion character at their acyl carbons[11b]. At which point of the rearrangement the 1,2-R shift is actually taking place remains open. It is conceivable that it occurs early on the rearrangement path, induced already by beginning oxygen attachment to Zr. It is less probable that R group migration has to await more or less complete Zr–C bond rupture and the formation of a five-membered ring carbene system similar to **32**, because **32** again is expected to be a high-energy species. 1,2-shifts in carbenes leading to olefin formation are of course well documented. In any case the two-step representation of Scheme 9 via **31** and **32** certainly is artificial, and the whole process of zirconocene enediolate formation should be summarized as in Scheme 11.

Scheme 11

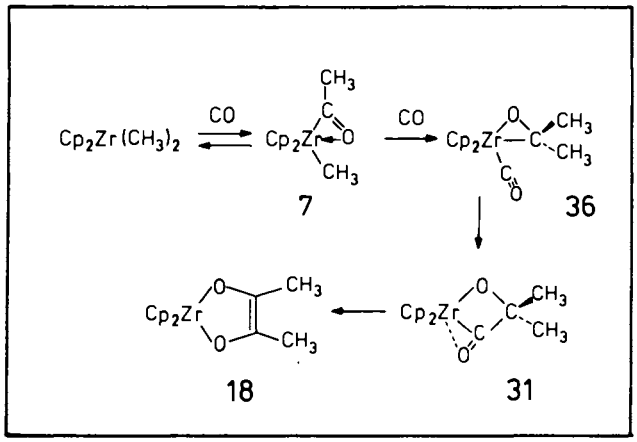

The keystep in this mechanism of intramolecular reductive CO coupling in d^0 early transition metal bis-organyl metallocenes is the formation of the CO-coordinated η^2-ketone (zirconaoxirane) intermediate **36** by CO-assisted (or generally: donor ligand-assisted) $COCH_3/CH_3$ (COR/R) coupling.

We have learned that the Bercaw group meanwhile has indeed isolated and characterized such species from carbonylation experiments of Cp^*_2 Hf- and Cp^*_2 Zr-derived hydridoalkyls while this study was independently conducted in our laboratory. The results of Bercaw et al. are shown in Scheme 12.

Scheme 12

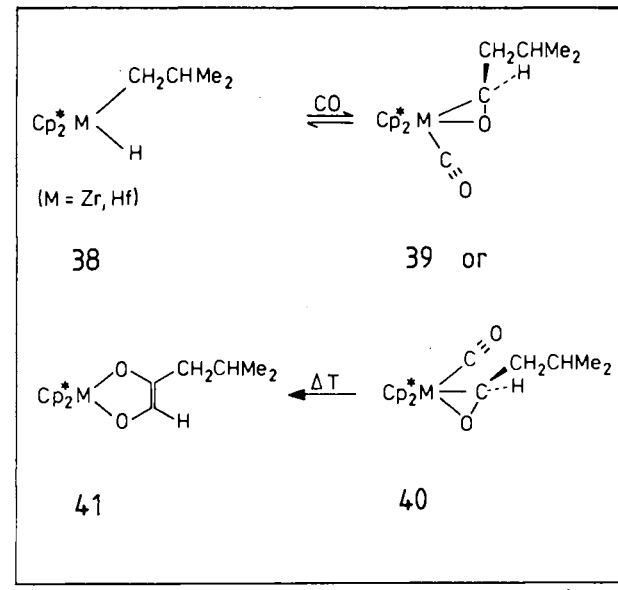

The fascinating details of this work will be published in a seperate paper[34], and we just mention here, that properly controlled carbonylation of hydridoalkyls **38** allows to isolate the moderately stable metallaoxirane carbonyls **39** or **40**[35], crucial to our theoretical mechanism above. At elevated temperature clean rearrangements of some of these compounds to the corresponding enediolate complexes take place, supporting strongly our theory-based mechanistic proposal.

Further Conclusions

A few points related to the reaction mechanism of enediolate formation deserve further comment.

1) The reader may ask why we neither have suggested nor performed a most obvious experiment to test the mechanism of Scheme 11. It would involve the generation of "Cp^*_2Zr" fragments from suitable precursor compounds in the presence of acetone *and* CO, intending to produce either **36** or **18** directly. "Cp^*_2Zr" or "Cp_2Zr" fragments can be easily generated, e.g. from Bercaw's dinitrogen complex $[Cp^*_2Zr(N_2)]_2N_2$[36] or by other routes[37], and such intermediates have found synthetic applications. It is well known, however[38], that ketones or aldehydes irreversibly and rapidly are coupled by "Cp^*_2Zr" or its analogs as shown in **42**, yielding saturated diolate complexes.

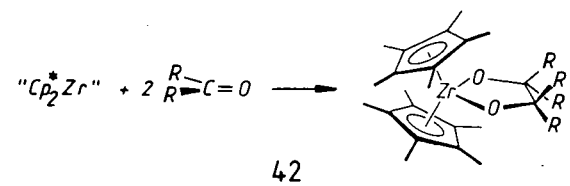

42

These coupling reactions, as for acetylenes[37], are symmetry-allowed exothermic processes and leave no chance to the enediolate pathway via **36** or its Cp* analog, if free acetone or other carbonyl compounds are available as reaction partners in addition to CO. Only if, as in Scheme 11, η^2-ketone (or η^2-aldehyde) ligands are exclusively formed within the coordination sphere of the metal, zirconaoxirane carbonyls like **36** can be formed. Free ketones or aldehydes would successfully compete with CO as reaction partners as soon as a first organic carbonyl compound is once bound to the metal fragment. This would inevitably lead to the outcome shown in **42**[39]. It would be interesting, however, to conduct Bercaw's enediolate forming carbonylation of $Cp^*_2Zr(CH_3)_2$ in the presence of free ketones or of labeled acetone to test whether they can suppress enediolate formation by taking over the role of the second CO in Scheme 11, giving diolate instead of enediolate complexes as products.

2) Our conclusions with respect to the necessity of a direct involvement of CO (or of a donor ligand in general) in the COR/R coupling step seem to contradict Erker's reaction of Scheme 8, where an η^2-benzophenone complex dimer is apparently formed without any additional nucleophile present. A monomolecular mechanism for the thermolysis of **26** to **27** is not unequivocally established yet, and an oxygen center of a second molecule could play the role of an electron donor to the Zr of the rearranging moiety here. More relevant in our context than the established intramolecular nature[40] of this reaction would therefore be experimental information about its molecularity. As the thermolysis of **26** is done at a temperature where dimer **27** itself produces the corresponding monomer in equilibrium, the presence of predominantly monomeric product immediately after thermolysis does not prove a monomolecular η^2-benzophenone complex formation without nucleophilic assistance. Furthermore, aryl to aroyl coupling may well be energetically quite different from an alkyl to acyl shift due to the π systems involved.

3) If carbon monoxide coordinates to the metal during the COR/R coupling process and thereby promotes the η^2-ketone formation, other 2-electron donors should do as well, provided that they do not attack the acyl carbon preferentially. A reflection of this may be Bercaw's and Roddick's observation[34] shown below.

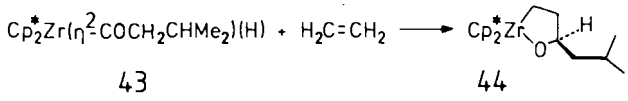

43 44

The acylhydride **43**, preformed at low temperature, reacts cleanly with ethene producing **44**, the oxidative coupling product of C_2H_4 and an aldehyde ligand. 2-Butyne reacts in the same manner. Intermediates analogous to the carbonyl complex **36** seem possible, although in this case the observed rates of reaction of the acyl hydrides qualitatively indicate unassisted hydride migration to the acyl group[41]. Kinetic as well as competition experiments with alkyl-acyl complexes would be interesting in order to establish whether alkenes or alkynes participate in the metallaoxirane-forming step. Erker's $Cp_2Zr(\eta^2$-benzophenone) dimer reacts with olefins to products which are analogous to **44**.

4) From our mechanistic picture it follows that the readiness of undergoing COR/R bond formation has to depend upon the electrophilicity of the acyl group. Lewis acids generally activate carbonyl groups by coordination to the oxygen end and therefore one would expect more facile η^2-ketone or η^2-aldehyde formation, if monoacyl species like **7** interact with suitable Lewis acids. This has indeed recently been oberved in elegant studies by Waymouth and Grubbs[42], who found facile Lewis acid promoted intramolecular coupling reactions of alkyl and acyl ligands in $Cp_2Zr(COR)(R)$ systems, giving zirconium ketone complexes **45**. Interestingly, the Lewis acids employed in these studies, e.g. AlR_2Cl, not only can bind to the oxygen of the starting compound $Cp_2Zr(\eta^2\text{-}COCH_3)(CH_3)$, but they also provide a halide ligand which can coordinate to the Zr center in the process of η^2-ketone formation (Scheme 13).

Scheme 13

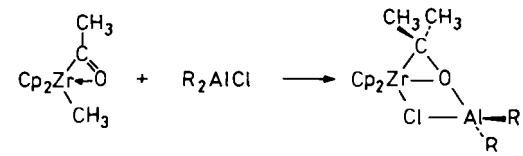

7 45

We have not studied the effect of oxygen-coordinating R_2AlCl Lewis acids upon the η^2-ketone-producing acyl-alkyl coupling step computationally as detailed as the process without Lewis acid participation described above. It is obvious, however, that any Lewis acid induced lowering of the acyl group's LUMO energy and any increase of the acyl carbon's electron deficiency and positive charge will facilitate acyl-alkyl coupling. In addition, Lewis acid coordination to the acyl oxygen will facilitate η^1-out-of-plane acyl orientations necessary for the alkyl to acyl shift. Model calculations with simple Lewis acids are presently being performed, and our preliminary results support the qualitative expectations.

5) Our discussion has predominantly focused upon electronic effects, concentrating upon one specific system with the Cp_2Zr metal fragment only. It should be stressed, that steric effects, be it within the metal fragment or within the ligand set, certainly play an immensely important role. The tendency to dimerize or to oligomerize, or to stay on mononuclear reaction pathways will depend heavily on sterics, i.e. upon the metal atom size, the choice of Cp or Cp* in the bent metallocene unit, and upon the steric requirements of COR and R groups. An a priori assessment of steric influences is very difficult, and steric demands often will alter the fine tuning of an electronic situation.

6) The mechanism derived for the Cp_2Zr fragment is not transferable to other metal fragments as templates for enediolate formation. We refer the reader to our earlier discussion of actinide systems[9], and we also note that replacing

Cp ligands with aryloxy groups changes the electronic situation drastically. According to mechanistic and kinetic results of the Rothwell group[10c] with intramolecular ligand coupling in isolable bis (η^2-iminoacyl) group 4 bis(aryloxy) complexes, enediolate forming in these systems very probably also does involve direct acyl-acyl coupling of bis(η^2-acyl) precursors (not isolated), in contrast to their group 4 metallocene congeners. The electronic differences between η^5-Cp (or Cp-derived) ligands and aryloxy groups can account for the accessibility of a bis-acyl coupling mechanism[43], which in its details is again subject to the same orbital symmetry requirements and geometric restrictions described in this paper and earlier for actinides[9].

Appendix: Computational Details

The molecular orbital calculations were of the Extended Hückel-type[44] with atomic parameters specified in Table 1. A modified Wolfsberg-Helmholz formula for computing the H_{ij} off-diagonal matrix elements[45] was used throughout.

Table 1. Atomic parameters used in the EH calculations

Orbital		H_{ii}[eV]	ζ_1	ζ_2	c_1[a]	c_2[a]
Zr	5s	−9.87	1.817			
	5p	−6.76	1.776			
	4d	−11.18	3.835	1.505	0.6211	0.5796
C	2s	−21.40	1.625			
	2p	−11.40	1.625			
O	2s	−32.30	2.275			
	2p	−14.80	2.275			
H	1s	−13.60	1.3			

[a] Coefficients used in the double-ζ-expansion.

In the calculations standardized model geometries were employed, adapted from the X-ray structure determinations of $Cp_2Zr(CH_3)(COCH_3)$[15b] and of **2**[24a]. Specific values were as follows:

Cp rings: local D_{5h}-symmetry, C−C = 140 pm, C−H = 108 pm; Cp_2Zr (C_{2v}): Zr−C_{Cp} = 250 pm, Cp−Zr−Cp = 130° (Cp rings eclipsed); Zr−C_{CH_3} = 233.6 pm, Zr−C_{COCH_3} = 219.7 pm, C=O_{Acyl} = 121 pm, [C=O_{Acyl} was set at 141 pm for the methyl to acetyl shift calculations (**I**−**IV**), as the carbonyl group C=O bond length has to elongate during the CC bond forming process], C_{CO}−CH_3 = 149.2 pm, C−H_{CH_3} = 110 pm, C−O of carbon monoxide = 114 pm, C=C of enediolate ring = 131.5 pm, Zr−O of enediolate complex = 204 pm, C−O of enediolate = 136.9 pm, C−CH_3 of enediolate = 152.5 pm; CH_3 groups: H−C−H = 109.47°; angles of enediolate ring: O−Zr−O = 79.2°, O−C=C = 118°, C=C−C_{CH_3} = 127°.

The bis-acetyl systems **12**−**17** in Scheme 6 were partially optimized with respect to their preferred acyl coordination mode at a fixed Cp_2Zr fragment for constant Zr−C_{COCH_3} bond distances of 219.7 pm and for rigid acetyl groups with O=C−C_{CH_3} angles of 120°. For an η^2-CH_3CO group the angle Zr−C=O was fixed at 70°, for an η^1-acetyl function at 120°. Then the angles between both Zr−C_{COCH_3} bond vectors and the C_{2v} axis of the Cp_2Zr fragment were optimized independently until the energetically best location of η^1- and η^2-coordinated acetyl groups within the mirror plane between the two Cp rings was reached. For the acetone complex **30** and related systems the following geometric parameters were used throughout: Zr−O = 210 pm, Zr−C = 230 pm, C−O = 145 pm, C−CH_3 = 152 pm, C−H = 110 pm, methyl groups tetrahedral; angle O−Zr−C = 38.14°, Zr−C−O = 63.44°, CH_3−C−CH_3 = 109.5°, CH_3−C−CH_3 plane "bent back" by 57°. These values were taken from available X-ray data of C−O-bound η^2-ketone, η^2-aldehyde, and η^2-ketene complexes in the literature[30] or, in part, were optimized. All other geometric details, in particular those related to geometry optimizations or to the modeling of reaction pathways, have been described in the main body of the paper as appropriate.

We are grateful to the *Fonds der Chemischen Industrie* and to the *Deutsche Forschungsgemeinschaft* (P. H., P. S., M. F.) for their support of this work. Discussions with Profs. *Bercaw, Buchwald, Erker, Grubbs,* and *Waymouth* were very helpful, and we would like to thank them in particular for disclosing experimental results to us prior to publication.

Experimental

All manipulations of Zr compounds were carried out under rigorously dry and oxygen-free conditions using an argon atmosphere and Schlenk techniques. All glassware was heated in vacuo prior to use. Whenever possible, Teflon valves, Teflon stopcocks, and greaseless joints with Teflon sleeves were employed for handling the zirconium compounds. All solvents were carefully purified and dried according to standard procedures[46] and were saturated with argon. – The mass spectra of Cp^*_2Zr-enediolate complexes obtained by carbonylation of $Cp^*_2Zr(CH_3)_2$, $Cp^*_2Zr(CD_3)_2$, and their 1:1 mixture were recorded using a Varian MAT 311 A instrument. Molecular ion peak isotope clusters were calculated using an appropriate PC program[47].

Pentamethylcyclopentadiene[48], $Cp^*_2ZrCl_2$[49], and $Cp^*_2Zr(CH_3)_2$[4a] were prepared as described in the literature. The deuterated compound $Cp^*_2Zr(CD_3)_2$ (**1-d$_6$**) was synthesized using CD_3Li, prepared from commercially available (99% D) CD_3I. As the dimethylzirconium compounds are light-sensitive both in solution and the solid state, their preparation, storage, and manipulation was done excluding light as far as possible. Carbonylation reactions were conducted as described by Bercaw[4a] with only slight modifications.

Carbonylation of $Cp^*_2Zr(CH_3)_2$ (**1**) *and $Cp^*_2Zr(CD_3)_2$* (**1-d$_6$**): 1.30 g of **1** (3.3 mmol) is dissolved in 80 ml of toluene in a 1-l round bottom flask with a teflon valve. After degassing the solution by means of a few freeze-and-thaw cycles the flask is flushed with carbon monoxide (1 atm) and heated to 65°C with vigorous magnetic stirring for ca. 15−20 h under CO gas. Then toluene is removed in vacuo, the red-violet solid residue is dissolved in the minimum amount of pentane, and the solution is transferred to a sublimation apparatus. Pentane is stripped off, and the product is sublimed (105°C, 10^{-4} Torr, ca. 12 h). Twofold recrystallization from pentane at −30°C yields 1.05 g (2.3 mmol, 70%) of the analytically pure enediolate complex **2**, which has been additionally characterized by an X-ray structure determination[24a] as published elsewhere.

1-d$_6$ was carbonylated in an identical manner yielding **2-d$_6$**.

Crossover Experiment: A solution of 0.627 g (1.60 mmol) of **1** and 0.636 g (1.60 mmol) of its deuterium analog **1-d$_6$** was carbonylated

using the same procedure as described above. The mass spectrum of an analytically pure sample of the resulting enediolate mixture showed the following isotopic distribution in its molecular ion peak: *m/z* (%) = 446 (53.9), 447 (24.5), 448 (22.4), 449 (5.2), 450 (18.1), 451 (5.7), 452 (44.9), 453 (20.3), 454 (17.0), 455 (4.0), 456 (13.9), 457 (3.1), 458 (2.1). This peak pattern is computed to be consistent with a 1:1 mixture of **2** and **2-d$_6$**, indicating clean intramolecular enediolate production with less than 0.5% crossover.

CAS Registry Numbers

1: 54039-38-2 / **2**: 67108-82-1 / CO: 630-08-0 / $Cp_2Zr(CH_3)_2$: 12636-72-5 / $Cp_2Zr(COCH_3)(CH_3)$: 60970-97-0

[1] [1a] J. Falbe, *Carbon Monoxide in Organic Synthesis*, Springer Verlag, Berlin 1970. – [1b] G. Henrici-Olivé, S. Olivé, *Coordination and Catalysis*, Verlag Chemie, Weinheim 1977. – [1c] J. P. Collmann, L. S. Hegedus, J. R. Norton, R. G. Finke, *Principles and Applications of Organotransition Metal Chemistry*, University Science Books, Mill Valley CA 1987. – [1d] G. W. Parshall, *Homogeneous Catalysis*, Wiley, New York 1980. – [1e] B. E. Kahn, R. D. Rieke, *Chem. Rev.* **88** (1988) 733.

[2] [2a] E. J. Kuhlmann, J. J. Alexander, *Coord. Chem. Rev.* **33** (1980) 195. – [2b] F. Calderazzo, *Angew. Chem.* **89** (1977) 305; *Angew. Chem. Int. Ed. Engl.* **16** (1977) 299. – [2c] G. Henrici-Olivé, S. Olivé, *Transition Met. Chem.* **1** (1976) 77. – [2d] A. Wojcicki, *Adv. Organomet. Chem.* **1973**, 87. – [2e] H. Berke, R. Hoffmann, *J. Am. Chem. Soc.* **100** (1978) 7224. – [2f] F. U. Axe, D. S. Marynick, *Organometallics* **6** (1987) 572. – [2g] N. Koga, K. Morokuma, *J. Am. Chem. Soc.* **108** (1986) 6136.

[3] [3a] P. Wolczanski, J. E. Bercaw, *Acc. Chem. Res.* **13** (1980) 121. – [3b] G. Erker, *Acc. Chem. Res.* **17** (1984) 103. – [3c] P. A. Bianconi, R. N. Vrtis, Ch. Pulla Rao, I. D. Williams, M. P. Engeler, S. J. Lippard, *Organometallics* **6** (1987) 1968. – [3d] D. H. Berry, J. E. Bercaw, A. J. Jircitano, K. B. Mertes, *J. Am. Chem. Soc.* **104** (1982) 4712. – [3e] B. Demerseman, R. Mahé, P. H. Dixneuf, *J. Chem. Soc., Chem. Commun.* **1984**, 1394. – See also ref.[1c].

[4] [4a] J. M. Manriquez, D. R. McAlister, R. D. Sanner, J. E. Bercaw, *J. Am. Chem. Soc.* **100** (1978) 2716. – [4b] A similar mechanism via a bis-carbene-like intermediate has been invoked in explaining C–C coupling of isocyanides with $Cp_2^*ZrH_2$: J. R. Bocarsly, C. Floriani, A. Chiesi-Villa, C. Guastini, *Organometallics* **5** (1986) 2380.

[5] C. McDade, J. E. Bercaw, *J. Organomet. Chem.* **279** (1985) 281.

[6] [6a] J. L. Petersen, J. W. Egan Jr., *Organometallics* **6** (1987) 2007. – [6b] Even olefinic groups in, e.g., $Cp_2^*Zr(CH=CHCH_3)_2$ react analogously (see ref.[5]) and do not yield 1,3-diene complexes as observed for $Cp_2Zr(CH=CH_2)_2$: R. Beckhaus, K.-H. Thiele, *J. Organomet. Chem.* **268** (1984) C7.

[7] D. A. Straus, *Ph. D. Thesis*, California Institute of Technology, 1983; R. H. Grubbs, personal communication.

[8] To our knowledge the potential of specifically synthesizing asymmetric acyloins or 1,2-diketones this way has not yet been explored.

[9] K. Tatsumi, A. Nakamura, P. Hofmann, R. Hoffmann, K. G. Moloy, T. J. Marks, *J. Am. Chem. Soc.* **108** (1986) 4467, and references therein.

[10] [10a] A. K. McMullen, I. P. Rothwell, J. C. Huffman, *J. Am. Chem. Soc.* **107** (1985) 1072, – [10b] S. L. Latesky, A. K. McMullen, I. P. Rothwell, J. C. Huffman, *Organometallics* **4** (1985) 1986. – [10c] L. R. Chamberlain, L. D. Durfee, P. E. Fanwick, L. M. Kobriger, S. L. Latesky, A. K. McMullen, B. D. Steffey, I. P. Rothwell, K. Folting, J. C. Huffman, *J. Am. Chem. Soc.* **109** (1987) 6068. – [10d] L. D. Durfee, A. K. McMullen, I. P. Rothwell, *J. Am. Chem. Soc.* **110** (1988) 1463.

[11] [11a] P. Hofmann, P. Stauffert, K. Tatsumi, A. Nakamura, R. Hoffman, *Organometallics* **4** (1985) 404. – [11b] K. Tatsumi, A. Nakamura, P. Hofmann, P. Stauffert, R. Hoffmann, *J. Am. Chem. Soc.* **107** (1985) 4440. – [11c] The regioselectivity of lateral CO insertion in $Cp_2Zr(CH_3)_2$ has meanwhile also been found in a Fenske-Hall MO study: L. Zhu, N. M. Kostic, *J. Organomet. Chem.* **335** (1987) 395. – [11d] Related is a recent GVB ab inito study of CO insertion into Sc–H bonds: A. K. Rappe, *J. Am. Chem. Soc.* **109** (1987) 5605.

[12] [12a] G. Erker, F. Rosenfeldt, *J. Organomet. Chem.* **188** (1980) C1. – [12b] G. Erker, F. Rosenfeldt, *Angew. Chem.* **90** (1978) 640; *Angew. Chem. Int. Ed. Engl.* **17** (1978) 605.

[13] No analogous η^2-acyl local minimum for "O-inside" emerges from the MO calculations; the existence of an η^1-coordination mode as a minimum structure on the potential surface of acyl to $Cp_2Zr(CH_3)$ coordination is theoretically well understood (viz. ref.[11]). It is a consequence of the nodal properties of acyl and metal fragment frontier MOs: P. Hofmann, P. Stauffert, N. E. Schore, *Chem. Ber.* **115** (1982) 2153.

[14] The energetic preference for 7 over **5** (both formally 18-electron systems) is overlap-based. In simple terms, **7** provides the stronger Zr to acyl-carbon bond (see ref.[11a,b]) for a detailed analysis).

[15] [15a] T. D. Tilley, *J. Am. Chem. Soc.* **107** (1985) 4084. – [15b] G. Fachinetti, G. Fochi, C. Floriani, *J. Chem. Soc., Dalton Trans.* **1977**, 1946. – [15c] J. A. Marsella, J. C. Huffman, K. G. Caulton, B. Longato, J. R. Norton, *J. Am. Chem. Soc.* **104** (1982) 6360. – $Cp_2Ti(\eta^2\text{-}COCH_3)Cl$, although not prepared by direct CO-insertion, has an analogous structure: – [15d] G. Fachinetti, C. Floriani, H. Stoeckli-Evans, *J. Chem. Soc., Dalton Trans.* **1977**, 2297.

[16] $Cp_2Zr(CH_3)_2$ undergoes enediolate formation experimentally. In contrast to Bercaw's Cp* derivative, however, carbonylation gives a dimer of the resulting enediolate complex: G. Erker, private communication.

[17] S. Gambarotta, C. Floriani, A. Chiesi-Villa, C. Guastini, *J. Am. Chem. Soc.* **105** (1983) 1690.

[18] [18a] B. D. Martin, S. A. Matchett, J. R. Norton, O. P. Anderson, *J. Am. Chem. Soc.* **107** (1985) 7952. – [18b] G. Erker, K. Kropp, C. Krüger, A.-P. Chiang, *Chem. Ber.* **115** (1982) 2447. – [18c] J. A. Marsella, J. C. Huffman, K. Folting, K. G. Caulton, *Inorg. Chim. Acta* **96** (1985) 161. – [18d] S. A. Matchett, J. R. Norton, O. P. Anderson, *Organometallics* **7** (1988) 228.

[19] Cases of a much less prohibitive nature of orbitally forbidden transformations in transition metal systems compared to organic molecules are known: [19a] J. Silvestre, *Nouv. J. Chim.* **12** (1988) 9. – [19b] R. T. Hembre, C. P. Scott, J. R. Norton, *J. Am. Chem. Soc.* **109** (1987) 3468.

[20] We have not optimized the intermediate η^2-η^1 structures with an out-of-plane η^1-acetyl. From $Cp_2Zr(\eta^1\text{-}COCH_3)(CH_3)$ studied earlier (viz. ref.[11a,b]) it was clear, that finding the lowest energy structure would have required very extensive geometry optimization including the Cp–Zr–Cp, C–Zr–C, Zr–C=O, O=C–CH_3 etc. angles. This was not considered necessary for our mechanistic conclusions.

[21] J. W. Lauher, R. Hoffmann, *J. Am. Chem. Soc.* **98** (1976) 1729.

[22] Energy surfaces were also calculated starting from an η^1-η^1 geometry **17** in an analogous manner as described in the text. As expected, the calculated barrier is approximately the sum of the **16**/**17** energy separation and the barrier for starting from **16** (η^2-η^2).

[23] [23a] This value is in remarkably good agreement with thermochemical estimates from recent data: L. E. Schock, T. J. Marks, *J. Am. Chem. Soc.* **110** (1988) 7701. – [23b] Even if we consider the calculated barrier to be only an upper limit due to incomplete geometry optimization, the energy difference of around 72 kcal/mol between **12** and the transition state of Figure 3 safely allows to discard acyl coupling as a viable reaction pathway.

[24] [24a] P. Hofmann, M. Frede, P. Stauffert, W. Lasser, U. Thewalt, *Angew. Chem.* **97** (1985) 693; *Angew. Chem. Int. Ed. Engl.* **24** (1985) 712. – [24b] H.-B. Bürgi, K. C. Dubler-Steudle, *J. Am. Chem. Soc.* **110** (1988) 4933.

[25] Lowered in energy by interactions with metal xz and yz AOs; it is this low-lying MO, which is responsible for the "carbenium-type" reactivity of η^2-acyl groups in such systems. See ref.[11b] for a detailed discussion.

[26] [26a] H.-B. Bürgi, J. D. Dunitz, B. Wipff, *Tetrahedron* **30** (1974) 1563. – [26b] C. L. Liotta, E. M. Burgess, W. H. Eberhardt, *J. Am. Chem. Soc.* **106** (1984) 4849, and references therein.

[27] [27a] G. Erker, U. Dorf, P. Czisch, J. L. Petersen, *Organometallics* **5** (1986) 668. – [27b] F. H. Elsner, T. D. Tilley, A. L. Rheingold, S. J. Geib, *J. Organomet. Chem.* **358** (1988) 169. – [27c] B. Hessen, J. H. Teuben, *J. Organomet. Chem.* **385** (1988) 135.

[28] G. Erker, P. Czisch, R. Schlund, K. Angermund, C. Krüger, *Angew. Chem.* **98** (1986) 356; *Angew. Chem. Int. Ed. Engl.* **25** (1986) 364.

[29] [29a] G. E. Herberich, J. Okuda, *Angew. Chem.* **97** (1985) 400; *Angew. Chem. Int. Ed. Engl.* **24** (1985) 402. – [29b] S. Gambarotta,

C. Floriani, A. Chiesi-Villa, C. Guastini, *J. Am. Chem. Soc.* **107** (1985) 2985.

[30] A collection of Zr–O–C three-membered ring structure data is available in ref.[27]. See also ref.[28] and ref.[18a] for related systems.

[31] For early waypoints of the methyl transfer itinerary (e.g. **I**–**III** with $C_{CH_3}-C_{COCH_3}$ distances between 306 and 226 pm), where the CH_3 group is still bonded mainly to zirconium, elongation of the $Zr-CH_3$ bond or rotation of the entire $C(O)(CH_3)$ moiety is of course highly unfavorable.

[32] These two MOs are typical for "pyramidal" d^0-Cp_2ML fragments like $Cp_2Zr(CH_3)^+$. They have been called d_π and d_σ and are described in detail in ref.[13].

[33] CO was allowed to move around Zr at 250 pm distance within the $Zr-C_{CH_3}-C_{COCH_3}$ plane.

[34] D. M. Roddick, J. E. Bercaw, *Chem. Ber.* **122** (1989) 1579, following paper in this issue.

[35] The CO ligand is labile and exchanges quickly with ^{13}CO; an X-ray structure determination in order to characterize the products as isomers **39** or **40** has not yet been possible: see ref.[34].

[36] [36a] J. M. Manriquez, J. E. Bercaw, *J. Am. Chem. Soc.* **96** (1974) 6229. – [37b] Hf analog: D. M. Roddick, M. D. Fryzuk, P. F. Seidler, G. L. Hillhouse, J. E. Bercaw, *Organometallics* **4** (1985) 97.

[37] W. A. Nugent, D. L. Thorn, R. L. Harlow, *J. Am. Chem. Soc.* **109** (1987) 2788.

[38] [38a] Relevant experiments are mentioned in ref.[21] of ref.[4a]. – [38b] M. Pasquali, C. Floriani, A. Chiesi-Villa, C. Guastini, *Inorg. Chem.* **20** (1981) 349.

[39] In view of related chemistry of $Cp_2Ti(CO)_2$ the alternative way of treating group 4 metallocene dicarbonyls with 1 equiv. of ketones or aldehydes does not seem promising either: T. L. Chen, T. H. Chan, A. Shaver, *J. Organomet. Chem.* **268** (1984) C1. – See also ref.[38b].

[40] G. Erker, F. Rosenfeldt, *J. Organomet. Chem.* **224** (1982) 29.

[41] A much more pronounced tendency for facile migration or coupling reactions of hydride as compared to alkyl in transition metal compounds is well known and understood: G. Parkin, E. Bunel, B. J. Burger, M. S. Trimmer, A. van Asselt, J. E. Bercaw, *J. Molecular Catal.* **41** (1987) 21.

[42] [42a] R. M. Waymouth, K. R. Klauser, R. H. Grubbs, *J. Am. Chem. Soc.* **108** (1986) 6385. – [42b] R. M. Waymouth, R. H. Grubbs, *Organometalics* 7 (1988) 1631.

[43] K. Tatsumi, paper to be published.

[44] R. Hoffmann, *J. Chem. Phys.* **39** (1963) 1397.

[45] [45a] R. Hoffmann, P. Hofmann, *J. Am. Chem. Soc.* **98** (1976) 598. – [45b] J. H. Ammeter, H.-B. Bürgi, J. C. Thibeault, R. Hoffmann, *J. Am. Chem. Soc.* **100** (1978) 3686.

[46] W. P. Fehlhammer, W. A. Herrmann, K. Öfele in *Handbuch der Präparativen Anorganischen Chemie* (G. Brauer, Ed.), 3rd ed., vol. III/3, p. 1802, Enke, Stuttgart 1981.

[47] Written and provided to us by A. Dengler, *Diplomarbeit*, Technische Universität München, 1986.

[48] F. X. Kohl, P. Jutzi, *J. Organomet. Chem.* **243** (1983) 119.

[49] J. M. Manriquez, D. R. McAlister, E. Rosenberg, A. M. Shiller, K. I. Williamson, S. I. Chan, J. E. Bercaw, *J. Am. Chem. Soc.*, **100** (1978) 3078.

[59/89]